# ON THE QUADRATIC FINITE ELEMENT APPROXIMATION OF 1-D WAVES: PROPAGATION, OBSERVATION AND CONTROL*

AURORA MARICA§ AND ENRIQUE ZUAZUA§†

**Abstract.** We study the *propagation*, *observation* and *control* properties of the *quadratic* $P_2$-*classical finite element* semi-discretization of the 1-d *wave equation* on a bounded interval. A careful Fourier analysis of the discrete wave dynamics reveals two different branches in the spectrum: the *acoustic* one, of physical nature, and the *optic* one, related to the perturbations that this second-order finite element approximation introduces with respect to the $P_1$-one. On both modes there are high frequencies with vanishing *group velocity* as the mesh size tends to zero. This shows that the classical property of continuous waves of being observable from the boundary fails to be uniform for this discretization scheme. As a consequence of this, the controls of the discrete waves may blow-up as the mesh size tends to zero. To remedy these high frequency pathologies, we design *filtering mechanisms* based on the *Fourier truncation* method or on a *bi-grid algorithm*, for which one can recover the uniformity of the observability constant in a finite time and, consequently, the possibility to control with uniformly bounded $L^2$ - controls appropriate projections of the solutions. This also allows showing that, by relaxing the control requirement, the controls are uniformly bounded and converge to the continuous ones as the mesh size tends to zero.

**Key words.** Quadratic finite element method, uniform mesh, vanishing group velocity, observability/controllability property, acoustic/optic mode, Fourier truncation method, bi-grid algorithm.

**AMS subject classifications.** 65J10, 65F08, 65N25, 65N30.

## 1. Introduction, problem formulation and main results.

Consider the 1-d *wave equation* with *non-homogeneous Dirichlet boundary conditions*:

$$\begin{cases} y_{tt}(x,t) - y_{xx}(x,t) = 0, \ x \in (0,1), \ t > 0, \\ y(0,t) = 0, \ y(1,t) = v(t), \ t > 0, \\ y(x,0) = y^0(x), \ y_t(x,0) = y^1(x), \ x \in (0,1). \end{cases} \tag{1.1}$$

System (1.1) is said to be *exactly controllable* in time $T \geq 2$ if, for all $(y^0, y^1) \in L^2 \times H^{-1}(0,1)$, there exists a control function $v \in L^2(0,T)$ such that the solution of (1.1) can be driven at rest at time $T$, i.e.

$$y(x,T) = y_t(x,T) = 0. \tag{1.2}$$

We also introduce the adjoint 1-d *wave equation* with *homogeneous Dirichlet boundary conditions*:

$$\begin{cases} u_{tt}(x,t) - u_{xx}(x,t) = 0, \ x \in (0,1), \ t > 0, \\ u(0,t) = u(1,t) = 0, \ t > 0, \\ u(x,T) = u^0(x), \ u_t(x,T) = u^1(x), \ x \in (0,1). \end{cases} \tag{1.3}$$

*Both authors were partially supported by Grants MTM2008-03541 and MTM2011-29306 of MICINN Spain, Project PI2010-04 of the Basque Government, ERC Advanced Grant FP7-246775 NUMERIWAVES and ESF Research Networking Programme OPTPDE. Additionally, the first author was supported by Grant PN-II-ID-PCE-2011-3-0075 of CNCS-UEFISCDI Romania.

§BCAM - Basque Center for Applied Mathematics, Alameda Mazarredo 14, 48009, Bilbao, Basque Country, Spain. Emails: marica@bcamath.org, zuazua@bcamath.org. Web pages: www.bcamath.org/en/people/marica, www.bcamath.org/en/people/zuazua.

†Ikerbasque - Basque Foundation for Science, Alameda Urquijo 36-5, Plaza Bizkaia, 48011, Bilbao, Basque Country, Spain.

This system is well-known to be well-posed in the *energy space* $\mathcal{V} := H_0^1 \times L^2(0,1)$ and the *total energy* below is conserved in time:

$$\mathcal{E}(u^0, u^1) := \frac{1}{2}(||u(\cdot,t)||^2_{H_0^1(0,1)} + ||u_t(\cdot,t)||^2_{L^2(0,1)}).$$

The *Hilbert Uniqueness Method* (HUM) introduced in [18] allows showing that the property of *exact controllability* for (1.1) is equivalent to the *boundary observability* of (1.3). The *observability property* of the wave equation ensures that the following *observability inequality* holds for all solutions of (1.3) provided $T \geq 2$:

$$\mathcal{E}(u^0, u^1) \leq C(T) \int_0^T |u_x(1,t)|^2 \, dt. \tag{1.4}$$

The best constant $C(T)$ in (1.4) is the so-called *observability constant*. The *observability time* $T$ has to be larger than the characteristic time $T^\star := 2$ which is needed by any solution associated to initial data $(u^0, u^1)$ supported in a very narrow neighborhood of $x = 1$ to travel along the *characteristic rays* $x(t) = x - t$, get to the boundary $x = 0$ and come back to the boundary $x = 1$ along the characteristics $x(t) = x + t$.

It is also well-known that, for all $T > 0$ and all solutions $u$ of the adjoint problem (1.3) with initial data $(u^0, u^1) \in \mathcal{V}$, the following *admissibility inequality* holds:

$$c(T) \int_0^T |u_x(1,t)|^2 \, dt \leq \mathcal{E}(u^0, u^1), \tag{1.5}$$

so that, for all $T \geq 2$, $||\partial_x u(1,\cdot)||_{L^2(0,T)}$ and $||(u^0, u^1)||_{\mathcal{V}}$ are equivalent norms.

As a consequence of these results, it is easy to see that for all $(y^0, y^1) \in L^2 \times H^{-1}(0,1)$, there exists a control $v \in L^2(0,T)$ driving the solution of (1.1) to the rest at $t = T$, i.e. such that (1.2) holds. This turns out to be equivalent to the fact that

$$\int_0^T v(t) u_x(1,t) \, dt = \langle (y^1, -y^0), (u(\cdot,0), u_t(\cdot,0)) \rangle_{\mathcal{V}',\mathcal{V}}, \tag{1.6}$$

for all solutions $u$ of (1.3), where $\langle \cdot, \cdot \rangle_{\mathcal{V}',\mathcal{V}}$ is the duality product between $\mathcal{V}' := H^{-1} \times L^2(0,1)$ and $\mathcal{V}$.

The HUM control $v$, the one of minimal $L^2(0,T)$-norm, has the explicit form

$$v(t) = \tilde{v}(t) := \tilde{u}_x(1,t), \tag{1.7}$$

where $\tilde{u}(x,t)$ is the solution corresponding to the minimum $(\tilde{u}^0, \tilde{u}^1) \in \mathcal{V}$ of the *quadratic functional*

$$\mathcal{J}(u^0, u^1) := \frac{1}{2} \int_0^T |u_x(1,t)|^2 \, dt - \langle (y^1, -y^0), (u(\cdot,0), u_t(\cdot,0)) \rangle_{\mathcal{V}',\mathcal{V}}. \tag{1.8}$$

An explicit expression of the optimal $L^2$-control $v$ in (1.1) in terms of the initial data $(y^0, y^1)$ is given in Theorem 3.1 in [13]. This result implies that, for any *piecewise linear* data $(y^0, y^1)$, the corresponding optimal control is a *piecewise quadratic* function and, in general, it is *discontinuous*.

The effect of substituting the continuous controlled wave equation (1.1) or the corresponding adjoint problem (1.3) by discrete models has been intensively studied during the last years, starting from some simple numerical schemes on *uniform meshes* like *finite differences* or *linear $P_1$-finite element* methods in [17] and, more recently, more complex schemes like the *discontinuous Galerkin* ones in [21]. In all these cases, the convergence of the approximation scheme in the classical sense of the numerical analysis does not suffice to guarantee that the sequence of discrete controls converges to the continuous ones. This is due to the fact that there are classes of initial data for the discrete adjoint problem generating *high frequency wave packets* propagating at a very low *group velocity* and that, consequently, are impossible to be observed from the boundary of the domain during a finite time, uniformly as the mesh-size parameter tends to zero. This leads to the divergence of the discrete observability constant as the mesh size tends to zero. High frequency pathological phenomena have also been observed for numerical approximation schemes of other models, like the linear Schrödinger equation (cf. [15]), in which one is interested in the uniformity of the so-called *dispersive estimates*, which play an important role in the study of the well-posedness of the corresponding non-linear models.

Several *filtering techniques* have been designed to face these high frequency pathologies: the *Fourier truncation method* (cf. [17]), which simply eliminates all the high frequency Fourier components propagating non-uniformly; the *bi-grid algorithm* introduced in [10] and [11] and rigorously studied in [16], [20] or [24] in the context of the finite difference semi-discretization of the 1-d and 2-d wave equation and of the Schrödinger equation (cf. [15]), which consists in taking initial data with slow oscillations obtained by linear interpolation from data given on a coarser grid; and the *numerical viscosity* method, which, by adding a suitable dissipative mechanism, damps out the spurious high frequencies ([23], [25]). We should emphasize that the *mixed finite element method* analyzed in [4] is, as far as we know, the unique method preserving the propagation and controllability properties of the continuous model uniformly in the mesh size parameter without requiring any extra filtering. The interested reader is referred to the survey articles [9] and [26] for a presentation of the development and the state of the art in this topic.

The purpose of the present paper is to analyze the behavior of the *quadratic $P_2$-finite element* semi-discretization of problems (1.1) and (1.3) from the uniform controllability/observability point of view. In **Section 2** we introduce in a rigorous way the discrete analogue of (1.1) and (1.3) and explain the minimization process generating the discrete controls. In **Section 3** we analyze the spectral problem associated to this discrete model and reveal the co-existence of two main types of Fourier modes: an *acoustic* one, of physical nature, related to the nodal components of the numerical solution, and an *optic* one, of spurious nature, related to the curvature with which the quadratic finite element method perturbs the linear approximation. We also study finer properties of the spectrum, for example the *spectral gap*, identifying three regions of null gap: the highest frequencies on both acoustic and optic modes and the lowest frequencies on the optic one. The content of this section is related to previously existing work. For instance, the dispersive properties of higher-order finite element methods have been analyzed in [1] in the setting of the Helmholtz equation. An explicit form of the acoustic dispersion relation was obtained for approximations of arbitrary order. It was shown that the numerical dispersion displays three different types of behavior, depending on the approximation order relative to the mesh-size and the wave number. In **Subsection 3.6** we explain how the Fourier analysis of the

numerical scheme in the 1-d case can be extended to the *biquadratic finite element* approximation of the 2-d wave equation in the square on uniform quadrilateral meshes. In **Section 4** we obtain some spectral identities allowing us to analyze the discrete observability inequality for the adjoint system. One of the main contributions of this paper is to design appropriate subspaces on which the observability constant is uniformly bounded as the mesh size parameter goes to zero. Thus, in **Section 5** we show that the *Fourier truncation* of the three pathological regions of the spectrum leads to an uniform observability inequality. In **Section 6** we prove that a filtering mechanism consisting in, firstly, considering *piecewise linear* initial data and, secondly, preconditioning the nodal components by a *bi-grid algorithm* guarantees uniform observability properties. Within the proof, we use a classical *dyadic decomposition argument* (cf. [16]), which mainly relies on the fact that for this class of initial data the total energy can be bounded by the energy of the projection on the low frequency components of the acoustic dispersion relation. We should emphasize that our results are finer than the ones in [6] or [7], where one obtains uniform observability properties for finite element approximations of any order, but by truncating the Fourier modes much under the critical scale $1/h$. Here we only consider the particular case of quadratic finite element approximation on 1-d meshes, but we get to the critical filtering scale $1/h$. Note however that the results in [6] and [7] apply in the more general context of *non-uniform grids* as well. In **Section 7** we present the main steps of the proof of the convergence of the discrete control problem under the assumption that the initial data in the corresponding adjoint problem are filtered through a *Fourier truncation* or a *bi-grid algorithm*. **Section 8** is devoted to present the conclusions of the paper and some related open problems.

**2. The $P_2$ - finite element approximation of 1-d waves.** For $p \in \mathbb{N}$, set $\mathbb{N}_p := [0,p] \cap \mathbb{N}$ and $\mathbb{N}_p^\star := [1,p] \cap \mathbb{N}$. Let $N \in \mathbb{N}$, $h = 1/(N+1)$ and $0 = x_0 < x_j < x_{N+1} = 1$ be the *nodes* of an *uniform grid* of the interval $[0,1]$, with $x_j = jh$, $j \in \mathbb{N}_{N+1}$, constituted by the subintervals $I_j = (x_j, x_{j+1})$, with $j \in \mathbb{N}_N$. We also define the *midpoints* $x_{j+1/2} = (j+1/2)h$ of this grid, with $j \in \mathbb{N}_N$. Let us introduce the space $\mathcal{P}_p(a,b)$ of polynomials of order $p$ on the interval $(a,b)$ and the *space of piecewise quadratic and continuous functions* $\mathcal{U}_h := \{u \in H_0^1(0,1) \text{ s.t. } u|_{I_j} \in \mathcal{P}_2(I_j),\ j \in \mathbb{N}_N\}$. The space $\mathcal{U}_h$ can be written as $\mathcal{U}_h = \text{span}\{\phi_j, j \in \mathbb{N}_N^\star\} \oplus \text{span}\{\phi_{j+1/2}, j \in \mathbb{N}_N\}$. Set $\chi_A$ to be the characteristic function of the set $A$. The two classes of *basis functions* are explicitly given below (see Fig. 2.1)

$$\phi_j(x) := \tfrac{2}{h^2}(x - x_{j-1/2})(x - x_{j-1})\chi_{I_{j-1}}(x) + \tfrac{2}{h^2}(x - x_{j+1/2})(x - x_{j+1})\chi_{I_j}(x)$$
$$\text{and} \qquad \phi_{j+1/2}(x) := -\tfrac{4}{h^2}(x - x_j)(x - x_{j+1})\chi_{I_j}(x).$$

The quadratic approximation of the adjoint problem (1.3) is as follows:

$$\begin{cases} u_h(\cdot,t) \in \mathcal{U}_h \text{ s.t. } \frac{d^2}{dt^2}(u_h(\cdot,t),\varphi)_{L^2(0,1)} + (u_h(\cdot,t),\varphi)_{H_0^1(0,1)} = 0,\ \forall \varphi \in \mathcal{U}_h, \\ u_h(x,T) = u_h^0(x), u_{h,t}(x,T) = u_h^1(x),\ x \in (0,1). \end{cases} \tag{2.1}$$

Since $u_h(\cdot,t) \in \mathcal{U}_h$, it admits the decomposition $u_h(x,t) = \sum_{j=1}^{2N+1} U_{j/2}(t)\phi_{j/2}(x)$. The function $u_h(\cdot,t)$ can be identified with the vector of its coefficients, $\mathbf{U}_h(t) := (U_{j/2}(t))_{j \in \mathbb{N}_{2N+1}^\star}$ (in the sequel, all vectors under consideration will be column vectors). Thus, using $\varphi = \phi_{j/2}$, $j \in \mathbb{N}_{2N+1}^\star$, as test functions in (2.1), system (2.1) can be written as the following system of $2N+1$ second-order differential equations (ODEs):

$$M_h \mathbf{U}_{h,tt}(t) + S_h \mathbf{U}_h(t) = 0,\ \mathbf{U}_h(T) = \mathbf{U}_h^0,\ \mathbf{U}_{h,t}(T) = \mathbf{U}_h^1, \tag{2.2}$$

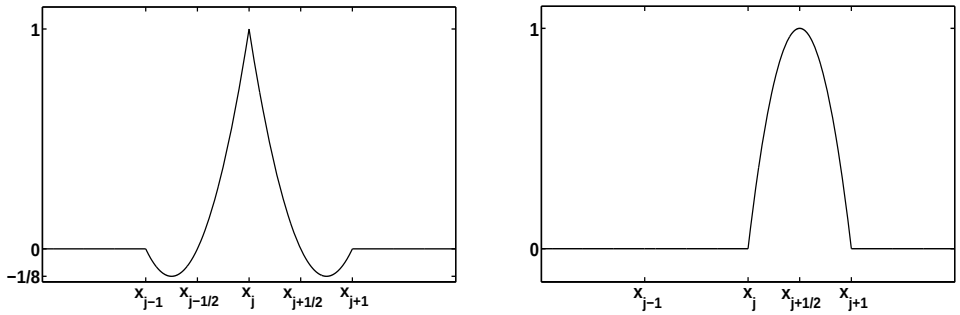


FIG. 2.1. *The basis functions: $\phi_j$ (left) and $\phi_{j+1/2}$ (right).*

where $M_h$ and $S_h$ are the following $(2N+1)\times(2N+1)$ *mass* and *stiffness* matrices alternating the *tridiagonal* and *pentadiagonal* structure:

$$M_h = \begin{pmatrix} \frac{8h}{15} & \frac{h}{15} & 0 & 0 & 0 & 0 & \cdots & 0 & 0 & 0 & 0 \\ \frac{h}{15} & \frac{4h}{15} & \frac{h}{15} & -\frac{h}{30} & 0 & 0 & \cdots & 0 & 0 & 0 & 0 \\ 0 & \frac{h}{15} & \frac{8h}{15} & \frac{h}{15} & 0 & 0 & \cdots & 0 & 0 & 0 & 0 \\ 0 & -\frac{h}{30} & \frac{h}{15} & \frac{4h}{15} & \frac{h}{15} & -\frac{h}{30} & \cdots & 0 & 0 & 0 & 0 \\ \cdots & \cdots & \ddots & \ddots & \ddots & \ddots & \ddots & \cdots & \cdots & \cdots & \cdots \\ 0 & 0 & 0 & 0 & 0 & 0 & \cdots & -\frac{h}{30} & \frac{h}{15} & \frac{4h}{15} & \frac{h}{15} \\ 0 & 0 & 0 & 0 & 0 & 0 & \cdots & 0 & 0 & \frac{h}{15} & \frac{8h}{15} \end{pmatrix}$$

and

$$S_h = \begin{pmatrix} \frac{16}{3h} & -\frac{8}{3h} & 0 & 0 & 0 & 0 & \cdots & 0 & 0 & 0 & 0 \\ -\frac{8}{3h} & \frac{14}{3h} & -\frac{8}{3h} & \frac{1}{3h} & 0 & 0 & \cdots & 0 & 0 & 0 & 0 \\ 0 & -\frac{8}{3h} & \frac{16}{3h} & -\frac{8}{3h} & 0 & 0 & \cdots & 0 & 0 & 0 & 0 \\ 0 & \frac{1}{3h} & -\frac{8}{3h} & \frac{14}{3h} & -\frac{8}{3h} & \frac{1}{3h} & \cdots & 0 & 0 & 0 & 0 \\ \cdots & \cdots & \ddots & \ddots & \ddots & \ddots & \ddots & \cdots & \cdots & \cdots & \cdots \\ 0 & 0 & 0 & 0 & 0 & 0 & \cdots & \frac{1}{3h} & -\frac{8}{3h} & \frac{14}{3h} & -\frac{8}{3h} \\ 0 & 0 & 0 & 0 & 0 & 0 & \cdots & 0 & 0 & -\frac{8}{3h} & \frac{16}{3h} \end{pmatrix}.$$

We introduce the discrete analogues of $H_0^1(0,1)$, $L^2(0,1)$ and $H^{-1}(0,1)$ as follows:

$$\mathcal{H}_h^i := \{\mathbf{F}_h = (F_{j/2})_{j\in\mathbb{N}^\star_{2N+1}} \in \mathbb{C}^{2N+1} \text{ s.t. } ||\mathbf{F}_h||_{h,i} < \infty\}, \quad i = -1, 0, 1.$$

For the elements of the space $\mathcal{H}_h^1$ we impose the additional requirement $F_0 = F_{N+1} = 0$. The *inner products* defining the discrete spaces $\mathcal{H}_h^i$, $i = -1, 0, 1$, are given by

$$(\mathbf{F}_h, \mathbf{G}_h)_{h,i} := ((M_h S_h^{-1})^{1-i} S_h \mathbf{F}_h, \mathbf{G}_h)_{\mathbb{C}^{2N+1}}$$

and the *norms* are given by $||\mathbf{F}_h||_{h,i}^2 := (\mathbf{F}_h, \mathbf{F}_h)_{h,i}$, for all $i = -1, 0, 1$. Here, $(\cdot,\cdot)_{\mathbb{C}^{2N+1}}$ is the inner product in the Euclidian space $\mathbb{C}^n$, defined by $(\mathbf{F}_h, \mathbf{G}_h)_{\mathbb{C}^{2N+1}} := \sum_{k=1}^{2N+1} F_{k/2}\overline{G}_{k/2}$ (the overline symbol denotes complex conjugation).

For $f_h \in \mathcal{U}_h$ of coefficients $\mathbf{F}_h = (F_{j/2})_{j\in\mathbb{N}^\star_{2N+1}} \in \mathcal{H}_h^1$, we introduce the following notations for the three possible *discrete derivatives* on each nodal point (the *forward*, the *backward* and the *midpoint* ones, represented by the $+$, $-$ and null superscripts):

$$\begin{aligned} \partial_h^{\pm} F_{j+1/2\mp1/2} = \partial_x f_h(x_{j+1/2\mp1/2}\pm) &= \mp\tfrac{F_{j+1/2\pm1/2} - 4F_{j+1/2} + 3F_{j+1/2\mp1/2}}{h}, \\ \partial_h F_{j+1/2} = \partial_x f_h(x_{j+1/2}) &= \tfrac{F_{j+1} - F_j}{h} \end{aligned} \tag{2.3}$$

and the values of $f_h$ at $x_{j+1/4} := (j+1/4)h$ and $x_{j+3/4} := (j+3/4)h$, $j \in \mathbb{N}_N$:

$$F_{j+1/2\pm 1/4} := f_h(x_{j+1/2\pm 1/4}) = \frac{3}{8}F_{j+1/2\pm 1/2} + \frac{3}{4}F_{j+1/2} - \frac{1}{8}F_{j+1/2\mp 1/2}.$$

With these notations, it is easy to check that the $||\cdot||_{h,1}$ and $||\cdot||_{h,0}$ - norms admit the following representations:

$$\begin{aligned} ||\mathbf{F}_h||^2_{h,1} &= \tfrac{h}{6}\sum_{j=0}^{N}\left(|\partial_h^+ F_j|^2 + 4|\partial_h F_{j+1/2}|^2 + |\partial_h^- F_{j+1}|^2\right), \\ ||\mathbf{F}_h||^2_{h,0} &= \tfrac{h}{90}\sum_{j=0}^{N}\Big(12|F_{j+1/2}|^2 + \sum_{\pm}\left(7|F_{j+1/2\pm 1/2}|^2 + 32|F_{j+1/2\pm 1/4}|^2\right)\Big). \end{aligned} \tag{2.4}$$

Set $\mathcal{V}_h := \mathcal{H}_h^1 \times \mathcal{H}_h^0$ and $\mathcal{V}_h' := \mathcal{H}_h^{-1} \times \mathcal{H}_h^0$ to be its dual. The *duality product* $\langle\cdot,\cdot\rangle_{\mathcal{V}_h',\mathcal{V}_h}$ between $\mathcal{V}_h'$ and $\mathcal{V}_h$ is defined as $\langle(\mathbf{F}_{h,1},\mathbf{G}_{h,1}),(\mathbf{F}_{h,2},\mathbf{G}_{h,2})\rangle_{\mathcal{V}_h',\mathcal{V}_h} := (\mathbf{F}_{h,1},\mathbf{F}_{h,2})_{h,0} + (\mathbf{G}_{h,1},\mathbf{G}_{h,2})_{h,0}$.

Problem (2.2) is well-posed in $\mathcal{H}_h^1 \times \mathcal{H}_h^0$. The *total energy* of its solutions is conserved in time:

$$\mathcal{E}_h(\mathbf{U}_h^0,\mathbf{U}_h^1) := \frac{1}{2}(||\mathbf{U}_h(t)||^2_{h,1} + ||\mathbf{U}_{h,t}(t)||^2_{h,0}). \tag{2.5}$$

One of the goals of this paper is to study discrete versions of the observability inequality (1.4) of the form

$$\mathcal{E}_h(\mathbf{U}_h^0,\mathbf{U}_h^1) \le C_h(T)\int_0^T ||B_h\mathbf{U}_h(t)||^2_{\mathbb{C}^{2N+1}}\,dt, \tag{2.6}$$

where $B_h$ is a $(2N+1)\times(2N+1)$ *observability matrix operator*. The observability inequality (2.6) makes sense for rather general matrices $B_h$, corresponding, for instance, to the observability from any open subset contained in the spatial domain $(0,1)$. But, within this paper, we focus on the particular case of *boundary observation operators* $B_h$, in the sense that they approximate the normal derivative $u_x(x,t)$ of the solution of the continuous adjoint problem (1.3) at $x=1$. The main example of such boundary matrix operators $B_h$ that will be used throughout this paper is as follows:

$$B_{ij} := \begin{cases} -\frac{1}{h}, & (i,j) = (2N+1, 2N), \\ 0, & \text{otherwise.} \end{cases} \tag{2.7}$$

The operator $B_h$ is also the one used for the finite difference semi-discretization in [17]. Let us remark that at the discrete level there are different ways to approximate the normal derivative of the continuous solution of (1.3). Since $B_h\mathbf{U}_h(t)$ is a vector and $u_x(x,t)$ is a scalar, the way in which $B_h\mathbf{U}_h(t)$ approximates $u_x(1,t)$ needs to be further explained. Remark that $B_h$ in (2.7) is almost a null matrix, excepting the penultimate component on the last row. The last component of $B_h\mathbf{U}_h(t)$, the only non-trivial one, equals to $u_{h,x}(x_{N+1/2},t)$. The consistency analysis shows that if $f$ is a sufficiently regular function and $f_h$ is its quadratic interpolation, then $f_{h,x}(x_{N+1/2})$ is a first-order approximation of $f_x(1)$.

We are interested in observability inequalities (2.6) in a finite, but sufficiently large observability time, say $T > T^\star > 0$. In this paper we show that, when working on the whole discrete space $\mathcal{V}_h \times \mathcal{V}_h$, the observability constant $C_h(T)$ blows-up as

$h \to 0$, whatever $T > 0$ is. More precisely, we design appropriate subspaces $\mathcal{S}_h \subset \mathcal{V}_h$ on which the observability constant $C_h(T)$ is uniformly bounded as $h \to 0$.

We will also prove that the discrete version of (1.5) below holds uniformly as $h \to 0$ in the whole approximate space $\mathcal{V}_h$, for all $T > 0$:

$$c_h(T) \int_0^T ||B_h \mathbf{U}_h(t)||^2_{\mathbb{C}^{2N+1}}\, dt \leq \mathcal{E}_h(\mathbf{U}_h^0, \mathbf{U}_h^1). \tag{2.8}$$

Once the observability problem is well understood, we are in conditions to address the *discrete control problem*. For a discrete control function $\mathbf{V}_h$ such that $B_h^* \mathbf{V}_h \in (\mathcal{H}_h^1)'$, we consider the following non-homogeneous problem:

$$M_h \mathbf{Y}_{h,tt}(t) + S_h \mathbf{Y}_h(t) = -B_h^* \mathbf{V}_h(t), \quad \mathbf{Y}_h(0) = \mathbf{Y}_h^0, \quad \mathbf{Y}_{h,t}(0) = \mathbf{Y}_h^1, \tag{2.9}$$

where $(\mathbf{Y}_h^1, \mathbf{Y}_h^0) \in \mathcal{V}_h'$. Here, the superscript $*$ denotes matrix transposition. Multiplying system (2.9) by any solution $\mathbf{U}_h(t)$ of the adjoint problem (2.2), integrating in time and imposing that at $t = T$ the solution is at rest, i.e.

$$\langle (\mathbf{Y}_{h,t}(T), -\mathbf{Y}_h(T)), (\mathbf{U}_h^0, \mathbf{U}_h^1) \rangle_{\mathcal{V}_h', \mathcal{V}_h} = 0, \ \forall (\mathbf{U}_h^0, \mathbf{U}_h^1) \in \mathcal{V}_h, \tag{2.10}$$

we obtain that $\mathbf{V}_h(t)$ necessarily satisfies the following identity which fully characterizes all possible exact controls $\mathbf{V}_h(t)$, for all $(\mathbf{U}_h^0, \mathbf{U}_h^1) \in \mathcal{V}_h$:

$$\int_0^T (\mathbf{V}_h(t), B_h \mathbf{U}_h(t))_{\mathbb{C}^{2N+1}}\, dt = \langle (\mathbf{Y}_h^1, -\mathbf{Y}_h^0), (\mathbf{U}_h(0), \mathbf{U}_{h,t}(0)) \rangle_{\mathcal{V}_h', \mathcal{V}_h}. \tag{2.11}$$

In view of this, we introduce the following discrete version of the *quadratic functional* (1.8) in which $\mathbf{U}_h(t)$ is the solution of the adjoint problem (2.2) with initial data $(\mathbf{U}_h^0, \mathbf{U}_h^1)$ and $(\mathbf{Y}_h^1, \mathbf{Y}_h^0) \in \mathcal{V}_h'$ is the initial data to be controlled in (2.9):

$$\mathcal{J}_h(\mathbf{U}_h^0, \mathbf{U}_h^1) = \frac{1}{2} \int_0^T ||B_h \mathbf{U}_h(t)||^2_{\mathbb{C}^{2N+1}}\, dt - \langle (\mathbf{Y}_h^1, -\mathbf{Y}_h^0), (\mathbf{U}_h(0), \mathbf{U}_{h,t}(0)) \rangle_{\mathcal{V}_h', \mathcal{V}_h}. \tag{2.12}$$

The functional $\mathcal{J}_h$ is *continuous* and *strictly convex*. Thus, provided it is coercive (which is actually what the uniform observability inequality guarantees), it has an unique minimizer $(\tilde{\mathbf{U}}_h^0, \tilde{\mathbf{U}}_h^1) \in \mathcal{S}_h$ whose *Euler-Lagrange equations* are as follows:

$$\int_0^T (B_h \tilde{\mathbf{U}}_h(t), B_h \mathbf{U}_h(t))_{\mathbb{C}^{2N+1}}\, dt = \langle (\mathbf{Y}_h^1, -\mathbf{Y}_h^0), (\mathbf{U}_h(0), \mathbf{U}_{h,t}(0)) \rangle_{\mathcal{V}_h', \mathcal{V}_h}, \tag{2.13}$$

for all $(\mathbf{U}_h^0, \mathbf{U}_h^1) \in \mathcal{S}_h$ and $\mathbf{U}_h(t)$ the corresponding solution of (2.2). The discrete HUM control is then

$$\mathbf{V}_h(t) = \tilde{\mathbf{V}}_h(t) := B_h \tilde{\mathbf{U}}_h(t). \tag{2.14}$$

Let us briefly comment the analogies between identities (1.7) and (2.14). As we said, when $B_h$ is a boundary observability matrix operator, like for example the one in (2.7), $B_h \tilde{\mathbf{U}}_h(t)$ is a vector whose last component $\tilde{v}_h(t)$, the only non-trivial one,

approximates the normal derivative of the solution to the adjoint continuous wave equation (1.3). Accordingly, the controls $-B_h^*\mathbf{V}_h(t)$ only act on $y_N(t)$ when $\mathbf{V}_h(t)$ is the numerical control obtained by (2.14). Consequently, the boundary observability operator $B_h$ does not act really at $x = 1$, but at $x = x_{N+1/2}$, being in fact an internal control acting on a single point which is closer and closer to the boundary as $h$ becomes smaller, so that in the limit as $h \to 0$ it becomes a boundary control.

Observe also that the control problem we deal with is a coupled system of non-homogeneous ODEs modeling the interaction between the nodal and the midpoint components. Thus, the node $x_{N+1/2}$ lies in fact on the boundary of the midpoint component. Consequently, the controls $-B_h^*\mathbf{V}_h(t)$ in (2.9), with $\mathbf{V}_h(t)$ as in (2.14), are really natural approximations of the continuous boundary controls $v$ in (1.1).

**3. Fourier analysis of the $P_2$-finite element method.** For the sake of completeness, we recall the spectral analysis of this $P_2$-finite element method, following [14]. The spectral problem associated to the adjoint system (2.1) is as follows:

$$\text{Find } (\Lambda_h, \tilde{\varphi}_h) \in \mathbb{R} \times \mathcal{U}_h \text{ such that } (\tilde{\varphi}_h, \phi_h)_{H_0^1} = \Lambda_h(\tilde{\varphi}_h, \phi_h)_{L^2},\ \forall \phi_h \in \mathcal{U}_h. \tag{3.1}$$

Due to the *symmetry* and the *coercivity* of the bi-linear forms generated by the scalar products $(\cdot,\cdot)_{L^2}$ and $(\cdot,\cdot)_{H_0^1}$, we have $\Lambda_h > 0$. Let $\tilde{\boldsymbol{\varphi}}_h = (\tilde{\varphi}_{j/2})_{j\in\mathbb{N}^\star_{2N+1}}$ be the components of the eigenfunction $\tilde{\varphi}_h$. The pair $(\Lambda_h, \tilde{\boldsymbol{\varphi}}_h)$ is a generalized eigensolution corresponding to the pair of matrices $(S_h, M_h)$, i.e.

$$S_h\tilde{\boldsymbol{\varphi}}_h = \Lambda_h M_h\tilde{\boldsymbol{\varphi}}_h. \tag{3.2}$$

Consider the normalized eigenvalues $\Lambda := h^2\Lambda_h$. System (3.2) is a pair of two equations:

$$-\frac{8}{3}\tilde{\varphi}_j + \frac{16}{3}\tilde{\varphi}_{j+1/2} - \frac{8}{3}\tilde{\varphi}_{j+1} - \Lambda\big(\frac{1}{15}\tilde{\varphi}_j + \frac{8}{15}\tilde{\varphi}_{j+1/2} + \frac{1}{15}\tilde{\varphi}_{j+1}\big) = 0, \tag{3.3}$$

for $j \in \mathbb{N}_N$, and

$$\begin{gathered}\tfrac{1}{3}\tilde{\varphi}_{j-1} - \tfrac{8}{3}\tilde{\varphi}_{j-1/2} + \tfrac{14}{3}\tilde{\varphi}_j - \tfrac{8}{3}\tilde{\varphi}_{j+1/2} + \tfrac{1}{3}\tilde{\varphi}_{j+1} - \\ -\Lambda\big(-\tfrac{1}{30}\tilde{\varphi}_{j-1} + \tfrac{1}{15}\tilde{\varphi}_{j-1/2} + \tfrac{4}{15}\tilde{\varphi}_j + \tfrac{1}{15}\tilde{\varphi}_{j+1/2} - \tfrac{1}{30}\tilde{\varphi}_{j+1}\big) = 0,\end{gathered} \tag{3.4}$$

depending on $j \in \mathbb{N}^\star_N$ and with the boundary condition $\tilde{\varphi}_0 = \tilde{\varphi}_{N+1} = 0$.

**3.1. The acoustic and optic modes.** From (3.3), we obtain that for $\Lambda \neq 10$, the values of $\tilde{\boldsymbol{\varphi}}_h$ at the midpoints can be obtained according to the two neighboring nodal values as follows:

$$\tilde{\varphi}_{j+1/2} = \frac{40+\Lambda}{8(10-\Lambda)}(\tilde{\varphi}_j + \tilde{\varphi}_{j+1}),\ \forall j \in \mathbb{N}_N. \tag{3.5}$$

Replacing (3.5) into (3.4), we obtain the following recurrence, for all $j \in \mathbb{N}^\star_N$:

$$-\frac{1}{2}\tilde{\varphi}_{j-1} + \frac{3\Lambda^2 - 104\Lambda + 240}{\Lambda^2 + 16\Lambda + 240}\tilde{\varphi}_j - \frac{1}{2}\tilde{\varphi}_{j+1} = 0, \text{ with } \tilde{\varphi}_0 = \tilde{\varphi}_{N+1} = 0. \tag{3.6}$$

It is easy to check that $\tilde{\varphi}_j = \sin(k\pi x_j)$ solves (3.6), for all $k \in \mathbb{N}^\star_N$,. Then the normalized eigenvalues $\Lambda$ verify the identity

$$\cos(k\pi h) = w(\Lambda), \text{ with } w(\Lambda) = \frac{3\Lambda^2 - 104\Lambda + 240}{\Lambda^2 + 16\Lambda + 240}. \tag{3.7}$$

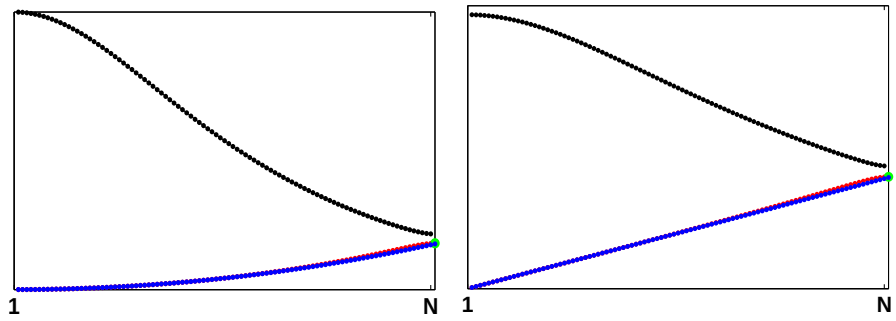


FIG. 3.1. *The eigenvalues $\Lambda_h$ (left) versus their square roots $\lambda_h$ (right): the continuous ones (blue) and the discrete acoustic/optic/resonant modes (red/black/green).*

For each $\eta \in [0, \pi]$, consider the second-order algebraic equation in $\Lambda = \Lambda(\eta)$:

$$(3 - \cos(\eta))\Lambda^2 - 2\Lambda(52 + 8\cos(\eta)) + 240(1 - \cos(\eta)) = 0, \tag{3.8}$$

whose solutions are $\Lambda = \Lambda^\alpha(\eta)$, $\alpha \in \{a, o\}$, with

$$\Lambda^\alpha(\eta) := \frac{22 + 8\cos^2(\eta/2) + 2\text{sign}(\alpha)\sqrt{\Delta(\eta)}}{1 + \sin^2(\eta/2)}, \tag{3.9}$$

$\text{sign}(a) = -1$, $\text{sign}(o) = 1$ and $\Delta(\eta) := 1 + 268\cos^2(\eta/2) - 44\cos^4(\eta/2)$. The superscript $a/o$ stands for *acoustic/optic*. We will also need the square roots of the Fourier symbols (3.9), the so-called *dispersion relations* for the discrete wave equation:

$$\lambda^a(\eta) := \sqrt{\Lambda^a(\eta)} \text{ and } \lambda^o(\eta) := \sqrt{\Lambda^o(\eta)}. \tag{3.10}$$

For each $k \in \mathbb{N}_N^\star$, set

$$\Lambda^{a,k} := \Lambda^a(k\pi h) \text{ and } \Lambda^{o,k} := \Lambda^o(k\pi h). \tag{3.11}$$

For $\alpha = a$ or $\alpha = o$, we refer to $(\Lambda^{\alpha,k})_{k\in\mathbb{N}_N^\star}$ as the *acoustic/optic branch* of the spectrum. The corresponding *eigenvectors* are as follows (with $j \in \mathbb{N}_{N+1}$ and, respectively, $j \in \mathbb{N}_N$ for the nodal/midpoint components):

$$\tilde\varphi_j^{\alpha,k} = \sin(k\pi x_j) \text{ and } \tilde\varphi_{j+1/2}^{\alpha,k} = \frac{40 + \Lambda^{\alpha,k}}{4(10 - \Lambda^{\alpha,k})}\cos\big(\frac{k\pi h}{2}\big)\sin(k\pi x_{j+1/2}). \tag{3.12}$$

**3.2. The resonant mode.** Up to this moment, we have explicitly calculated $2N$ solutions of the eigenvalue problem (3.2). To do this, we have supposed that $\Lambda \neq 10$. But $\Lambda = \Lambda^r := 10$ is also an eigenvalue corresponding to the *resonant* mode, the superscript $r$ standing for *resonant*. The components of the corresponding eigenvector $\tilde{\boldsymbol{\varphi}}_h^r$ are

$$\tilde\varphi_j^r = 0, \ \forall j \in \mathbb{N}_{N+1}, \text{ and } \tilde\varphi_{j+1/2}^r = (-1)^j, \ \forall j \in \mathbb{N}_N. \tag{3.13}$$

For any normalized eigenvalue $\Lambda$, set $\Lambda_h = \Lambda/h^2$, $\lambda = \sqrt{\Lambda}$, $\lambda_h = \sqrt{\Lambda_h}$ (Fig. 3.1).

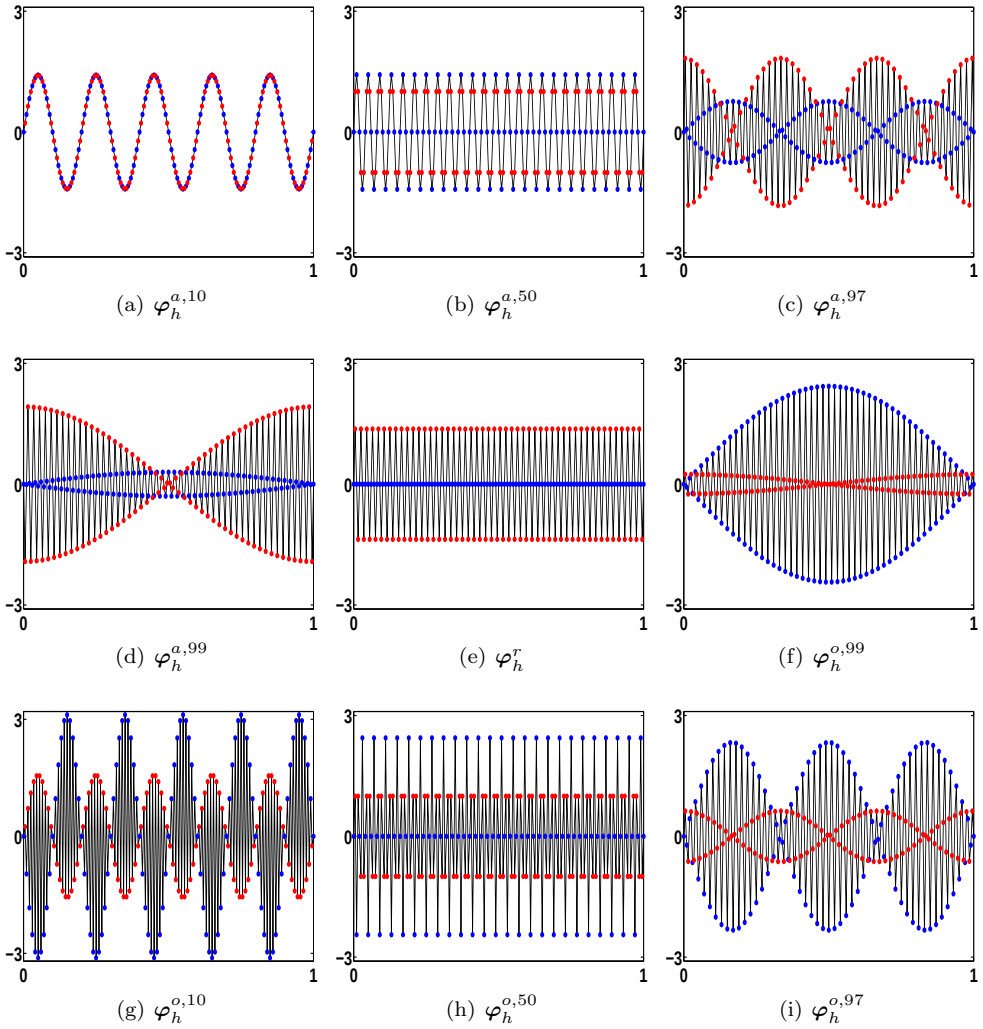

(a) $\boldsymbol{\varphi}_h^{a,10}$ (b) $\boldsymbol{\varphi}_h^{a,50}$ (c) $\boldsymbol{\varphi}_h^{a,97}$

(d) $\boldsymbol{\varphi}_h^{a,99}$ (e) $\boldsymbol{\varphi}_h^{r}$ (f) $\boldsymbol{\varphi}_h^{o,99}$

(g) $\boldsymbol{\varphi}_h^{o,10}$ (h) $\boldsymbol{\varphi}_h^{o,50}$ (i) $\boldsymbol{\varphi}_h^{o,97}$

FIG. 3.2. *Examples of normalized acoustic, optic and resonant eigenvectors for $N = 99$. In blue/red, we represent their nodal/midpoint components.*

**3.3. Normalized eigenvectors.** For any eigenvector $\tilde{\boldsymbol{\varphi}}_h \in \{\tilde{\boldsymbol{\varphi}}_h^{a,k},\ \tilde{\boldsymbol{\varphi}}_h^{o,k},\ k \in \mathbb{N}_N^\star,\ \tilde{\boldsymbol{\varphi}}_h^{r}\}$, we define the $L^2$-normalized eigenvector $\boldsymbol{\varphi}_h := \tilde{\boldsymbol{\varphi}}_h / ||\tilde{\boldsymbol{\varphi}}_h||_{h,0}$.

Using the expression (2.4) of the discrete norms $||\cdot||_{h,0}$ and $||\cdot||_{h,1}$ and the identity (3.5), we obtain the following representations of the $||\cdot||_{h,0}$ and $||\cdot||_{h,1}$-norms of the acoustic and optic eigenvectors in terms of their nodal components:

$$||\tilde{\boldsymbol{\varphi}}_h^{\alpha,k}||_{h,0}^2 = \frac{1}{24}\Big[1+\frac{500}{|10-\Lambda^{\alpha,k}|^2}\Big]h\sum_{j=0}^{N}|\tilde{\varphi}_{j+1}^{\alpha,k}+\tilde{\varphi}_j^{\alpha,k}|^2+\frac{h}{12}\sum_{j=0}^{N}|\tilde{\varphi}_{j+1}^{\alpha,k}-\tilde{\varphi}_j^{\alpha,k}|^2, \quad (3.14)$$

for all $\alpha \in \{a, o\}$ and $k \in \mathbb{N}_N^\star$, and

$$||\tilde{\boldsymbol{\varphi}}_h^{\alpha,k}||_{h,1}^2 = h\sum_{j=0}^{N}\Big|\frac{\tilde{\varphi}_{j+1}^{\alpha,k}-\tilde{\varphi}_j^{\alpha,k}}{h}\Big|^2+\frac{1}{h^2}\frac{4}{3}\Big|\frac{5\Lambda^{\alpha,k}}{4(10-\Lambda^{\alpha,k})}\Big|^2 h\sum_{j=0}^{N}|\tilde{\varphi}_{j+1}^{\alpha,k}+\tilde{\varphi}_j^{\alpha,k}|^2. \quad (3.15)$$

Then, using the representation formula (3.14), the identities

$$\begin{array}{c} h\sum_{j=0}^{N}\sin^2(k\pi x_j)=\frac{1}{2},\quad h\sum_{j=0}^{N}|\sin(k\pi x_{j+1})-\sin(k\pi x_j)|^2=2\sin^2\left(\frac{k\pi h}{2}\right),\\ h\sum_{j=0}^{N}|\sin(k\pi x_{j+1})+\sin(k\pi x_j)|^2=2\cos^2\left(\frac{k\pi h}{2}\right),\forall k\in\mathbb{N}_N^\star, \end{array} \tag{3.16}$$

and (3.7), we obtain

$$||\tilde{\boldsymbol{\varphi}}_h^{\alpha,k}||_{h,0}^2=\frac{1}{3\tilde{W}(\Lambda^{\alpha,k})},\ \text{with}\ \tilde{W}(\Lambda)=\frac{(\Lambda-10)(\Lambda^2+16\Lambda+240)}{19\Lambda^2+120\Lambda-3600}. \tag{3.17}$$

Let us remark that $||\tilde{\boldsymbol{\varphi}}_h^{a,k}||_{h,0}$ blows-up as $kh\to 1$. With the above notation,

$$\varphi_j^{\alpha,k}=n^{\alpha,k}\sin(k\pi x_j)\ \text{and}\ \varphi_{j+1/2}^{\alpha,k}=m^{\alpha,k}\sin(k\pi x_{j+1/2}),\ \forall\alpha\in\{a,o\}, \tag{3.18}$$

where $n$ and $m$ stand for the *nodal* and *midpoint* components and

$$n^{\alpha,k}=\sqrt{3\tilde{W}(\Lambda^{\alpha,k})},\quad m^{\alpha,k}=n^{\alpha,k}\frac{40+\Lambda^{\alpha,k}}{4(10-\Lambda^{\alpha,k})}\cos\left(\frac{k\pi h}{2}\right).$$

Using the explicit form of the $||\cdot||_{h,0}$-norm and the characterization (3.13) of the resonant mode, we obtain $||\tilde{\boldsymbol{\varphi}}_h^r||_{h,0}^2=8/15$ and therefore, the normalized resonant mode $\boldsymbol{\varphi}_h^r$ satisfies

$$\varphi_j^r=0,\ \forall j\in\mathbb{N}_{N+1}\ \text{and}\ \varphi_{j+1/2}^r=(-1)^j\sqrt{15/8},\ \forall j\in\mathbb{N}_N. \tag{3.19}$$

Let us introduce the sets of *eigenvalues* and of $\mathcal{H}_h^0$-normalized *eigenfunctions*, i.e.

$$\mathcal{EV}_h=\{(\Lambda_h^{\alpha,k})_{(\alpha,k)\in\{a,o\}\times\mathbb{N}_N^\star},\ \Lambda_h^r\}\ \text{and}\ \mathcal{EF}_h=\{(\boldsymbol{\varphi}_h^{\alpha,k})_{(\alpha,k)\in\{a,o\}\times\mathbb{N}_N^\star},\ \boldsymbol{\varphi}_h^r\}. \tag{3.20}$$

**3.4. Fourier representation of discrete solutions.** Since $\mathcal{EF}_h$ is an orthonormal basis in $\mathcal{H}_h^0$, the initial data in (2.2) admit the following *Fourier representation*, in which $\widehat{u}^{\alpha,k,i}:=(\mathbf{U}_h^i,\boldsymbol{\varphi}_h^{\alpha,k})_{h,0}$ and $\widehat{u}^{r,i}:=(\mathbf{U}_h^i,\boldsymbol{\varphi}_h^r)_{h,0}$:

$$\mathbf{U}_h^i=\sum_{k=1}^{N}\sum_{\alpha\in\{a,o\}}\widehat{u}^{\alpha,k,i}\boldsymbol{\varphi}_h^{\alpha,k}+\widehat{u}^{r,i}\boldsymbol{\varphi}_h^r,\quad\forall i=0,1. \tag{3.21}$$

Correspondingly, the solution of (2.2) can be represented as follows:

$$\mathbf{U}_h(t)=\sum_{\pm}\Big[\sum_{k=1}^{N}\sum_{\alpha\in\{a,o\}}\widehat{u}_\pm^{\alpha,k}\exp(\pm it\lambda_h^{\alpha,k})\boldsymbol{\varphi}_h^{\alpha,k}+\widehat{u}_\pm^r\exp(\pm it\lambda_h^r)\boldsymbol{\varphi}_h^r\Big], \tag{3.22}$$

where

$$\widehat{u}_\pm^{\alpha,k}=\frac{1}{2}\Big(\widehat{u}^{\alpha,k,0}\pm\frac{\widehat{u}^{\alpha,k,1}}{i\lambda_h^{\alpha,k}}\Big),\forall\alpha\in\{a,o\},\ k\in\mathbb{N}_N^\star,\quad\widehat{u}_\pm^r=\frac{1}{2}\Big(\widehat{u}^{r,0}\pm\frac{\widehat{u}^{r,1}}{i\lambda_h^r}\Big).$$

The *total energy* (2.5) of the solutions of (2.2) is then as follows:

$$\mathcal{E}_h(\mathbf{U}_h^0,\mathbf{U}_h^1)=\sum_{k=1}^{N}\sum_{\alpha\in\{a,o\}}\Lambda_h^{\alpha,k}(|\widehat{u}_+^{\alpha,k}|^2+|\widehat{u}_-^{\alpha,k}|^2)+\Lambda_h^r(|\widehat{u}_+^r|^2+|\widehat{u}_-^r|^2). \tag{3.23}$$

**3.5. Limits and monotonicity of the eigenvalues.** Firstly, we remark that, as $kh \to 1$, $\Lambda^{a,k} \to 10$, $\Lambda^{o,k} \to 12$ and, as $kh \to 0$, $\Lambda^{o,k} \to 60$. On the other hand, the first-order derivatives of the Fourier symbols (3.9) or of the corresponding dispersion relations (3.10), the so-called *group velocities*, verify the positivity conditions below:

$$\partial_\eta \lambda^a(\eta),\ \partial_\eta \Lambda^a(\eta),\ -\partial_\eta \lambda^o(\eta),\ -\partial_\eta \Lambda^o(\eta) > 0,\ \forall \eta \in (0,\pi),$$

meaning that the *acoustic/optic branch is strictly increasing/decreasing* in $k$. Consequently, the high frequency wave packets involving only the acoustic or the optic modes and concentrated around a given frequency $k^\star \in \mathbb{N}_N^\star$ propagate in opposite directions. Moreover, at $\eta = 0$ or $\eta = \pi$, the group velocities satisfy

$$\partial_\eta \Lambda^\alpha(\pi) = \partial_\eta \Lambda^\alpha(0) = 0, \quad \partial_\eta \lambda^\alpha(\pi) = \partial_\eta \lambda^o(0) = 0,\ \forall \alpha \in \{a,o\},\ \text{and } \partial_\eta \lambda^a(0) = 1,$$

which, according to the analysis in [21], shows, in particular, that there are waves concentrated on each mode which propagate at arbitrarily slow velocity.

**3.6. Extension to biquadratic finite element approximations of waves on quadrilateral meshes of the square.** Let $N_x, N_y \in \mathbb{N}$, $h_x := 1/(N_x+1)$ and $h_y := 1/(N_y+1)$ be the *mesh sizes* in the $x$ and $y$ directions and $(x_{j_x}, y_{j_y}) := (j_x h_x, j_y h_y)$, $j_x \in \mathbb{N}_{N_x+1}$, $j_y \in \mathbb{N}_{N_y+1}$, be the *nodes* of the *uniform grid* of the square $[0,1]\times[0,1]$ constituted by the *cells* $I_{j_x,j_y} := [x_{j_x}, x_{j_x+1}] \times [y_{j_y}, y_{j_y+1}]$, with $j_x \in \mathbb{N}_{N_x}$, $j_y \in \mathbb{N}_{N_y}$. We also define the *midpoints* $(x_{j_x+1/2}, y_{j_y+1/2}) := ((j_x+1/2)h_x, (j_y+1/2)h_y)$ (with $j_x \in \mathbb{N}_{N_x}$, $j_y \in \mathbb{N}_{N_y}$), $(x_{j_x}, y_{j_y+1/2})$ and $(x_{j_x+1/2}, y_{j_y})$. Set $\mathcal{U}_{h_x,h_y} := \{u \in H_0^1([0,1]\times[0,1])$ s.t. $u(\cdot,a) \in \mathcal{U}_{h_x}$ and $u(a,\cdot) \in \mathcal{U}_{h_y}, \forall a \in (0,1)\}$ to be the *space of biquadratic functions*. Its elements are *piecewise quadratic* and *continuous* functions in both horizontal and vertical directions. This space can be written as $\mathcal{U}_{h_x,h_y} = \text{span}\{\phi_{j_x/2,j_y/2}, j_x \in \mathbb{N}^\star_{2N_x+1},\ j_y \in \mathbb{N}^\star_{2N_y+1}\}$, where the basis functions are given by $\phi_{j_x/2,j_y/2}(x,y) := \phi_{j_x/2}(x)\phi_{j_y/2}(y)$ (see Fig. 3.3).

The *biquadratic semi-discretization* of the *wave equation on the unit square* with *homogeneous Dirichlet boundary conditions* is similar to (2.1), in which $\mathcal{U}_h$ is replaced by $\mathcal{U}_{h_x,h_y}$. Since the solution $u_{h_x,h_y}$ belongs to $\mathcal{U}_{h_x,h_y}$, it admits the decomposition $u_{h_x,h_y}(x,y,t) = \sum_{j_x=1}^{2N_x+1}\sum_{j_y=1}^{2N_y+1} U_{j_x/2,j_y/2}(t)\phi_{j_x/2,j_y/2}(x,y)$. We organize the unknowns into a vector $\mathbf{U}_{h_x,h_y}(t)$ of $(2N_x+1)\times(2N_y+1)$ components obtained by concatenating the $2N_y+1$ vectors $\mathbf{U}_{\cdot,k/2}(t) := (U_{j/2,k/2})_{j\in\mathbb{N}^\star_{2N_x+1}}$ of dimension $2N_x+1$, so that $\mathbf{U}_{h_x,h_y}(t) := (\mathbf{U}_{\cdot,k/2}(t))_{k\in\mathbb{N}^\star_{2N_y+1}}$. In this way, we obtain the second-order system of ODEs $M_{h_x,h_y}\partial_t^2 \mathbf{U}_{h_x,h_y}(t) + S_{h_x,h_y}\mathbf{U}_{h_x,h_y}(t) = 0$, in which the *mass* and *stiffness* matrices are defined by $M_{h_x,h_y} := M_{h_y} \otimes M_{h_x}$ and $S_{h_x,h_y} := M_{h_y} \otimes S_{h_x} + S_{h_y} \otimes M_{h_x}$. Here, $M_h$ and $S_h$ are the *mass* and *stiffness* matrices in the 1-d context and $A \otimes B$ is the *Kronecker product* of the matrices $A$ and $B$ (cf. [12], equation 2.1). The matrices $M_{h_x,h_y}$ and $S_{h_x,h_y}$ alternate the *block pentadiagonal* and *block tridiagonal* structures.

Let us now consider the *spectral problem* associated to the biquadratic finite element approximation of waves, $S_{h_x,h_y}\boldsymbol{\varphi}_{h_x,h_y} = \Lambda_{h_x,h_y} M_{h_x,h_y}\boldsymbol{\varphi}_{h_x,h_y}$. Using the expressions of the mass/stiffness matrices in the 2-d case as Kronecker products of matrices in the 1-d case and the property that $(A\otimes B)(\mathbf{a}\otimes\mathbf{b}) = A\mathbf{a}\otimes B\mathbf{b}$ for any square matrices $A, B$ and any column vectors $\mathbf{a}, \mathbf{b}$ of dimensions $m$ and $n$ (see equation 2.4 in [12]), we can easily check that $\boldsymbol{\varphi}_{h_x,h_y} := \boldsymbol{\varphi}_{h_y} \otimes \boldsymbol{\varphi}_{h_x}$ and $\Lambda_{h_x,h_y} := \Lambda_{h_x} + \Lambda_{h_y}$, where $(\Lambda_{h_x}, \boldsymbol{\varphi}_{h_x})$ and $(\Lambda_{h_y}, \boldsymbol{\varphi}_{h_y})$ are any two solutions of the 1-d spectral problem (3.2) with $h = h_x$ and $h = h_y$. For $\xi, \eta \in [0,\pi]$ and $\alpha, \beta \in \{a,o\}$ (standing for *acoustic/optic* mode in the 1-d case), we define the corresponding *Fourier symbols* of the discrete

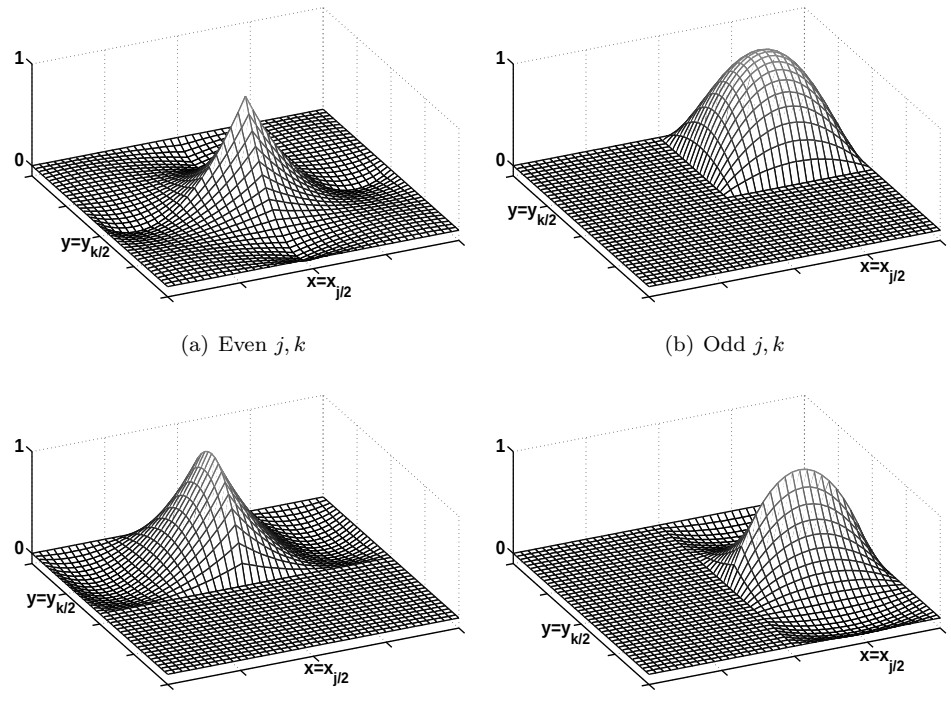


(a) Even $j, k$ (b) Odd $j, k$

(c) Even $j$, odd $k$ (d) Odd $j$, even $k$

FIG. 3.3. *Basis functions $\phi_{j/2,k/2}$ generating the biquadratic finite element space $\mathcal{U}_{h_x,h_y}$*

2-d Laplacian as $\Lambda^{\alpha,\beta}(\xi,\eta) := \Lambda^\alpha(\xi) + \Lambda^\beta(\eta)$ and $\lambda^{\alpha,\beta}(\xi,\eta) := \sqrt{\Lambda^{\alpha,\beta}(\xi,\eta)}$ to be the corresponding *dispersion relations* for the wave equation. The associated *group velocity* $|\nabla_{(\xi,\eta)}\lambda^{\alpha,\beta}(\xi,\eta)|$ is as follows:

$$|\nabla_{(\xi,\eta)}\lambda^{\alpha,\beta}(\xi,\eta)|^2 := \frac{|\lambda^\alpha(\xi)|^2|\partial_\xi\lambda^\alpha(\xi)|^2 + |\lambda^\beta(\eta)|^2|\partial_\eta\lambda^\beta(\eta)|^2}{|\lambda^\alpha(\xi)|^2 + |\lambda^\beta(\eta)|^2}.$$

It vanishes at some point $(\xi,\eta)$ if and only if $\partial_\xi\lambda^\alpha(\xi) = \partial_\eta\lambda^\beta(\eta) = 0$, or if $\partial_\xi\lambda^\alpha(\xi) = \lambda^\beta(\eta) = 0$, or if $\lambda^\alpha(\xi) = \partial_\eta\lambda^\beta(\eta) = 0$. More precisely, when $\alpha = \beta = a$, the critical points are $(\xi,\eta) \in \{(\pi,0),(0,\pi),(\pi,\pi)\}$, whereas, when $(\alpha,\beta) \in \{(a,o),(o,a),(o,o)\}$, they are $(\xi,\eta) \in \{(0,0),(\pi,0),(0,\pi),(\pi,\pi)\}$ (see Fig. 3.4).

**4. Boundary observability of eigenvectors.** The main result of this section is as follows:

PROPOSITION 4.1. *For all $\alpha \in \{a,o\}$ and all $k \in \mathbb{N}_N^\star$, the following identity holds for both acoustic and optic eigensolutions:*

$$||\boldsymbol{\varphi}_h^{\alpha,k}||_{h,1}^2 = \frac{|\varphi_N^{\alpha,k}|^2}{h^2 W(\Lambda^{\alpha,k})},\ W(\Lambda) = \frac{24(\Lambda-10)^2(\Lambda-12)(\Lambda-60)}{(-19\Lambda^2-120\Lambda+3600)(\Lambda^2+16\Lambda+240)}. \quad (4.1)$$

*Moreover, for the resonant mode, the following identity holds:*

$$||\boldsymbol{\varphi}_h^r||_{h,1}^2 = \frac{16}{3}\left|\frac{\varphi_{N+1/2}^r}{h}\right|^2. \quad (4.2)$$

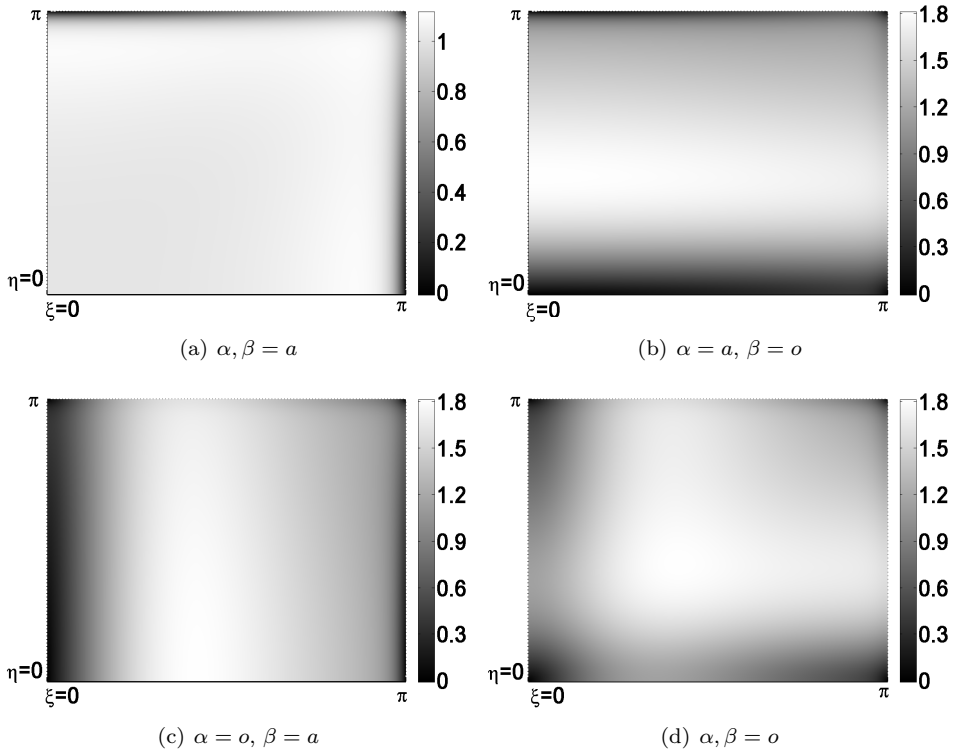


(a) $\alpha, \beta = a$ (b) $\alpha = a$, $\beta = o$

(c) $\alpha = o$, $\beta = a$ (d) $\alpha, \beta = o$

FIG. 3.4. *Level set representation of the group velocity* $|\nabla_{(\xi,\eta)}\lambda^{\alpha,\beta}(\xi,\eta)|$ *for the biquadratic approximation of the wave equation. In black, the points where this group velocity vanishes.*

*Remark 1. The identity (4.1) is the discrete analogue of the continuous one* $||\varphi^k||^2_{H_0^1} = |\varphi^k_x(1)|^2/2$, *where* $\varphi^k(x) = \sqrt{2}\sin(k\pi x)$ *is the* $L^2$*-normalized eigenfunction corresponding to the eigenvalue* $\Lambda^k = k^2\pi^2$.

*Remark 2. Due to the monotonicity of the Fourier symbols, we get* $\Lambda^{a,k} \in (0, 10)$ *and* $\Lambda^{o,k} \in (12, 60)$, *for all* $k \in \mathbb{N}^\star_N$. *The quadratic equation* $-19x^2 - 120x + 3600 = 0$ *has the roots* $x_1 = -60(1 + \sqrt{20})/19 < 0$ *and* $x_2 = 60/(1 + \sqrt{20}) \in (10, 12)$. *This implies that* $W(\Lambda) > 0$, *for all* $\Lambda \in (0, 10) \cup (12, 60)$.

*Remark 3. Due to the fact that the numerator of* $W(\Lambda)$ *in (4.1) vanishes for* $\Lambda = 10$, $\Lambda = 12$ *and* $\Lambda = 60$ *and to the above lower and upper bounds of the Fourier symbols, we deduce that the coefficient* $1/W(\Lambda^{\alpha,k})$ *of* $|\varphi^{\alpha,k}_N/h|^2$ *in (4.1) converges to infinity as* $kh \to 1$ *both when* $\alpha = a$ *or* $\alpha = o$ *and as* $kh \to 0$ *when* $\alpha = o$.

*Proof of Proposition 4.1.* Fix $\alpha \in \{a, o\}$ and $k \in \mathbb{N}^\star_N$. Obviously, it is enough to prove (4.1) for the un-normalized eigenvectors $\tilde{\boldsymbol{\varphi}}^{\alpha,k}_h$. We will use two approaches to prove the identity (4.1). The first one consists on using the classical multiplier $x_j(\tilde{\varphi}_{j+1} - \tilde{\varphi}_{j-1})/2h$ (which is a discrete version of the continuous one $x\varphi_x$) in the spectral problem (3.6) and then to apply the *Abel summation by parts formula*

$$\sum_{j=1}^{N}(a_{j+1} - a_j)b_j = a_{N+1}b_{N+1} - a_1b_0 - \sum_{j=0}^{N} a_{j+1}(b_{j+1} - b_j), \tag{4.3}$$

for all $(a_j)_{j\in\mathbb{N}^\star_{N+1}} \in \mathbb{C}^{N+1}$ and $(b_j)_{j\in\mathbb{N}_{N+1}} \in \mathbb{C}^{N+2}$. In what follows, we will add the superscript $\alpha, k$ to the solution $\tilde{\boldsymbol{\varphi}}_h$ of (3.6). In this way, we deduce the following identity, with $w$ as in (3.7):

$$\frac{h}{2}\sum_{j=0}^{N}\left|\tilde\varphi_{j+1}^{\alpha,k}\pm\tilde\varphi_j^{\alpha,k}\right|^2=\frac{1}{2}\left|\tilde\varphi_N^{\alpha,k}\right|^2+(w(\Lambda^{\alpha,k})\pm 1)h\sum_{j=0}^{N}\tilde\varphi_{j+1}^{\alpha,k}\tilde\varphi_j^{\alpha,k}.$$

By replacing the crossed sum $h\sum_{j=0}^{N}\tilde\varphi_{j+1}^{\alpha,k}\tilde\varphi_j^{\alpha,k}$ obtained from the above identity corresponding to the + sign into the one with the − sign, we get:

$$h\sum_{j=0}^{N}\left|\frac{\tilde\varphi_{j+1}^{\alpha,k}-\tilde\varphi_j^{\alpha,k}}{h}\right|^2=\frac{2|\tilde\varphi_N^{\alpha,k}|^2}{h^2\big(w(\Lambda^{\alpha,k})+1\big)}+\frac{1}{h^2}\frac{w(\Lambda^{\alpha,k})-1}{w(\Lambda^{\alpha,k})+1}h\sum_{j=0}^{N}\left|\tilde\varphi_{j+1}^{\alpha,k}+\tilde\varphi_j^{\alpha,k}\right|^2. \quad (4.4)$$

Using the representation (3.15) of the $||\cdot||_{h,1}$-norm of the optic and acoustic eigenvectors in terms of the nodal components, we obtain that (4.4) is equivalent to

$$\begin{aligned}||\tilde{\boldsymbol{\varphi}}_h^{\alpha,k}||_{h,1}^2&=\tfrac{2|\tilde\varphi_N^{\alpha,k}|^2}{h^2\left(w(\Lambda^{\alpha,k})+1\right)}+\tfrac{f(\Lambda^{\alpha,k})}{h}\sum_{j=0}^{N}\left|\tilde\varphi_{j+1}^{\alpha,k}+\tilde\varphi_j^{\alpha,k}\right|^2,\\ &\text{with}\quad f(\Lambda):=\tfrac{w(\Lambda)-1}{w(\Lambda)+1}+\tfrac{25\Lambda^2}{12(10-\Lambda)^2}.\end{aligned} \quad (4.5)$$

By replacing (3.14) into (3.15), we obtain the following identity:

$$\begin{aligned}||\tilde{\boldsymbol{\varphi}}_h^{\alpha,k}||_{h,1}^2&=\tfrac{12}{h^2}||\tilde{\boldsymbol{\varphi}}_h^{\alpha,k}||_{h,0}^2+\tfrac{g(\Lambda^{\alpha,k})}{h}\sum_{j=0}^{N}\left|\tilde\varphi_{j+1}^{\alpha,k}+\tilde\varphi_j^{\alpha,k}\right|^2,\\ &\text{with}\quad g(\Lambda):=\tfrac{25\Lambda(\Lambda-12)}{12(\Lambda-10)^2}-\tfrac{\Lambda-60}{2(\Lambda-10)}.\end{aligned} \quad (4.6)$$

On the other hand, by multiplying by $\tilde{\boldsymbol{\varphi}}_h$ in (3.2), we obtain the following relation between the $||\cdot||_{h,0}$ and $||\cdot||_{h,1}$-norms of the eigenvectors:

$$||\tilde{\boldsymbol{\varphi}}_h^{\alpha,k}||_{h,1}^2=\frac{\Lambda^{\alpha,k}}{h^2}||\tilde{\boldsymbol{\varphi}}_h^{\alpha,k}||_{h,0}^2. \quad (4.7)$$

By replacing (4.7) into (4.6), we get

$$h\sum_{j=0}^{N}\left|\tilde\varphi_{j+1}^{\alpha,k}+\tilde\varphi_j^{\alpha,k}\right|^2=\frac{\Lambda^{\alpha,k}-12}{\Lambda^{\alpha,k}g(\Lambda^{\alpha,k})}h^2||\tilde{\boldsymbol{\varphi}}_h^{\alpha,k}||_{h,1}^2. \quad (4.8)$$

By combining (4.5) and (4.8), we obtain the identity below, from which (4.1) follows immediately:

$$\Big[1-\frac{\Lambda^{\alpha,k}-12}{\Lambda^{\alpha,k}}\frac{f(\Lambda^{\alpha,k})}{g(\Lambda^{\alpha,k})}\Big]||\tilde{\boldsymbol{\varphi}}_h^{\alpha,k}||_{h,1}^2=\frac{2}{w(\Lambda^{\alpha,k})+1}\left|\frac{\tilde\varphi_N^{\alpha,k}}{h}\right|^2.$$

The second approach to prove (4.1) is much more direct. It consists in using the representation (3.15) of the $||\cdot||_{h,1}$-norm of the eigenvectors, the trigonometric identities (3.16), the fact that $|\tilde\varphi_N^{\alpha,k}|=|\sin(k\pi h)|$ and the relation (3.7). Thus, for $w$ as in (3.7) and $W$ as in (4.1), we get:

$$\frac{h^2||\tilde{\boldsymbol{\varphi}}_h^{\alpha,k}||_{h,1}^2}{|\tilde\varphi_N^{\alpha,k}|^2}=\frac{1-w(\Lambda^{\alpha,k})+\frac{4}{3}\left|\frac{5\Lambda^{\alpha,k}}{4(10-\Lambda^{\alpha,k})}\right|^2(1+w(\Lambda^{\alpha,k}))}{(1-w(\Lambda^{\alpha,k}))(1+w(\Lambda^{\alpha,k}))}=\frac{1}{W(\Lambda^{\alpha,k})}.$$

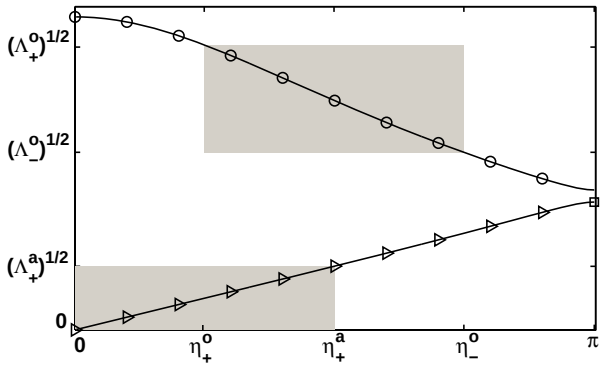


FIG. 5.1. *The selected area contains square roots of eigenvalues whose eigenvectors generate the truncated class $\mathcal{T}_{h,\eta_+^a,\eta_-^o,\eta_+^o}$. With triangle/circle/square-shaped markers, the acoustic/optic/resonant mode.*

The identity (4.2) follows by combining the explicit expressions (3.13) of the components of the resonant eigenvector and (2.4). This concludes the proof of (4.2). □

## 5. Discrete observability inequality: an Ingham approach.

**5.1. The observability inequality.** In this section we prove that the discrete observability inequality (2.6) holds uniformly as $h \to 0$ in a truncated class of initial data, with the observation operator $B_h$ as in (2.7). More precisely, consider $0 < \Lambda_+^a < 10$ and $12 < \Lambda_-^o \leq \Lambda_+^o < 60$ and correspondingly the wave numbers

$$\eta_+^a := (\Lambda^a)^{-1}(\Lambda_+^a) \text{ and } \eta_\pm^o := (\Lambda^o)^{-1}(\Lambda_\pm^o). \tag{5.1}$$

Set $I^a := [0, \eta_+^a]$, $I^o := [\eta_+^o, \eta_-^o]$ and introduce the subspace of $\mathbb{C}^{2N+1}$ given by

$$\mathcal{T}_{h,\eta_+^a,\eta_-^o,\eta_+^o} := \text{span}\{\boldsymbol{\varphi}_h^{a,k}, k\pi h \in I^a\} \oplus \text{span}\{\boldsymbol{\varphi}_h^{o,k}, k\pi h \in I^o\}.$$

Consider the truncated subspace $\mathcal{S}_h \subset \mathcal{V}_h$ defined by (see also Fig. 5.1):

$$\mathcal{S}_h := (\mathcal{T}_{h,\eta_+^a,\eta_-^o,\eta_+^o} \times \mathcal{T}_{h,\eta_+^a,\eta_-^o,\eta_+^o}) \cap \mathcal{V}_h. \tag{5.2}$$

The main result of this subsection is as follows:

THEOREM 5.1. *For all $\Lambda_+^a \in (0, 10)$ and $\Lambda_-^o \leq \Lambda_+^o \in (12, 60)$ independent of $h$, all initial data $(\mathbf{U}^{h,0}, \mathbf{U}^{h,1}) \in \mathcal{S}_h$, with $\mathcal{S}_h$ as in (5.2) and $\eta_+^a$, $\eta_\pm^o$ given by (5.1), and for any observability time $T > T^\star_{\eta_+^a,\eta_-^o,\eta_-^a}$, with*

$$T^\star_{\eta_+^a,\eta_-^o,\eta_-^a} := \frac{2}{\min\{\min_{\eta\in I^a} \partial_\eta \lambda^a(\eta), \min_{\eta\in I^o}(-\partial_\eta \lambda^o(\eta))\}},$$

*the observability inequality (2.6), with $B_h$ as in (2.7), holds uniformly as $h \to 0$.*

*Proof of Theorem 5.1.* The fact that the eigenmodes involved in the class $\mathcal{T}_{h,\eta_+^a,\eta_-^o,\eta_+^o}$ are such that the gap in each branch has a strictly positive lower bound, uniformly as $h \to 0$, allows us to apply Ingham Theorem (cf. [19], Theorem 4.3, pp. 59). More

precisely, the spectral gap on each branch $(\lambda_h^{\alpha,k})_{1\le k\le N}$, with $\alpha\in\{a,o\}$, is bounded as follows:

$$\lambda_h^{\alpha,k+1}-\lambda_h^{\alpha,k}\ge \pi\min_{\eta\in I^\alpha}|\partial_\eta\lambda^\alpha(\eta)|>0,\quad \forall k \text{ s.t. } k\pi h,(k+1)\pi h\in I^\alpha.$$

Then $\gamma=\gamma(\eta_+^a,\eta_-^o,\eta_+^o):=\pi\min\{\min_{\eta\in I^a}\partial_\eta\lambda^a(\eta),\min_{\eta\in I^o}(-\partial_\eta\lambda^o(\eta))\}>0$ is the uniform gap needed to apply the Ingham theory. From (3.22) and the definition of the class $\mathcal{T}_{h,\eta_+^a,\eta_-^o,\eta_+^o}$, we get

$$U_N(t)=\sum_{\pm}\sum_{\alpha\in\{a,o\}}\sum_{k\pi h\in I^\alpha}\widehat{u}_\pm^{\alpha,k}\exp(\pm it\lambda_h^{\alpha,k})\varphi_N^{\alpha,k}.$$

By applying the *inverse inequality* in Ingham Theorem (cf. [19], pp. 60, (4.9)), we can guarantee that, for all $T>2\pi/\gamma=T^\star_{\eta_+^a,\eta_-^o,\eta_+^o}$, there exists a constant $C_-(T)>0$ independent of $h$ such that

$$C_-(T)\sum_{\pm}\sum_{\alpha\in\{a,o\}}\sum_{k\pi h\in I^\alpha}|\widehat{u}_\pm^{\alpha,k}|^2\Big|\frac{\varphi_N^{\alpha,k}}{h}\Big|^2\le\int_0^T\Big|\frac{U_N(t)}{h}\Big|^2dt.$$

Using the identities (4.1) and $||\boldsymbol{\varphi}_h^{\alpha,k}||_{h,1}^2=\Lambda_h^{\alpha,k}$, we obtain the inequality below (in which $W$ is as in (4.1)):

$$C_-(T)\sum_{\pm}\sum_{\alpha\in\{a,o\}}\sum_{k\pi h\in I^\alpha}\Lambda_h^{\alpha,k}|\widehat{u}_\pm^{\alpha,k}|^2W(\Lambda^{\alpha,k})\le\int_0^T\Big|\frac{U_N(t)}{h}\Big|^2dt.$$

Taking into account that for the filtering algorithm under consideration $\Lambda\in[0,\Lambda_+^a]\cup[\Lambda_-^o,\Lambda_+^o]\subset[0,10)\cup(12,60)$ (with uniform inclusion as $h\to0$ due to the fact that $\Lambda_+^a$ and $\Lambda_\pm^o$ do not depend on $h$), and that for $\Lambda\in[0,10)\cup(12,60)$, the weight $W$ is strictly positive, we can guarantee that

$$C_-(\eta_+^a,\eta_-^o,\eta_+^o):=\min_{\Lambda\in[0,\Lambda_+^a)\cup(\Lambda_-^o,\Lambda_+^o)}W(\Lambda)\text{ is strictly positive.}$$

Then the proof concludes by taking in (2.6) (with $B_h$ as in (2.7)) the observability constant $C_h(T):=C_-(T)C_-(\eta_+^a,\eta_-^o,\eta_+^o)$, which is independent of $h$. □

**5.2. The admissibility inequality.** Using the *direct inequality* in Ingham Theorem (cf. [19], pp. 60, (4.8)), we can also prove that inequality (2.8) (with $B_h$ as in (2.7)) holds uniformly as $h\to0$, for all $T>0$, with $c_h(T):=1/(C_+(T)C_+(\eta_+^a,\eta_-^o,\eta_+^o))$, where $C_+(T)$ is the constant of the direct Ingham inequality and $C_+(\eta_+^a,\eta_-^o,\eta_+^o)$ below is bounded:

$$C_+(\eta_+^a,\eta_-^o,\eta_+^o):=\max_{\Lambda\in[0,\Lambda_+^a)\cup(\Lambda_-^o,\Lambda_+^o)}W(\Lambda).$$

## 6. Discrete observability inequality: a bi-grid algorithm.

**6.1. The observability inequality.** In this section, $N$ is an *odd* number. We consider the space $\mathcal{L}_h$ containing discrete *piecewise linear functions* given below

$$\mathcal{L}_h:=\{\mathbf{F}_h=(F_{j/2})_{j\in\mathbb{N}^\star_{2N+1}},\ F_0=F_{N+1}=0,\ F_{j+1/2}=(F_j+F_{j+1})/2,\ \forall j\in\mathbb{N}_N\}$$

and the space $\mathcal{B}_h$ of functions whose *nodal components* are given by a *bi-grid algorithm*, i.e. the *even* components are arbitrarily given and the *odd* ones are computed as average of the two even neighboring values:

$$\mathcal{B}_h := \{\mathbf{F}_h = (F_{j/2})_{j\in\mathbb{N}^\star_{2N+1}}, F_0 = F_{N+1} = 0,\ F_{2j+1} = (F_{2j}+F_{2j+2})/2,\ \forall j \in \mathbb{N}_{(N-1)/2}\}.$$

We also define the subspace $\mathcal{S}_h$ of $\mathcal{V}_h$

$$\mathcal{S}_h := ((\mathcal{L}_h \cap \mathcal{B}_h) \times (\mathcal{L}_h \cap \mathcal{B}_h)) \cap \mathcal{V}_h. \tag{6.1}$$

The aim of this section is to prove that the observability inequality (2.6) still holds uniformly as $h \to 0$ for initial data in the bi-grid subspace $\mathcal{S}_h$ in (6.1):

THEOREM 6.1. *For all $T > 2$ and all initial data $(\mathbf{U}_h^0, \mathbf{U}_h^1)$ in the adjoint problem (2.2) belonging to $\mathcal{S}_h$ introduced in (6.1), the observability inequality (2.6) with $B_h$ given by (2.7) holds uniformly as $h \to 0$.*

*Remark 4. Note that, in the bi-grid filtering mechanism we have designed, the data under consideration have been taken, before filtering through the classical bi-grid algorithm, to be piecewise linear in each interval $(x_j, x_{j+1})$, $j \in \mathbb{Z}$, which imposes a further restriction. This allows to obtain the sharp observability time.*

*The bi-grid filtering algorithm proposed in Theorem 6.1 yields optimal observability time, i.e. the characteristic one $T^\star = 2$. This is due to the fact that for a numerical scheme the minimal time required for the observability to hold is $2/v$, where $v$ is the minimal group velocity involved in the corresponding solution. From our analysis, we will see that the bi-grid filtering algorithm above acts mainly as a Fourier truncation of the whole optic diagram and of the second half (the high frequency one) of the acoustic one. Consequently, $v := \min_{\eta\in[0,\pi/2]} \partial_\eta\lambda^a(\eta)$. Since the group velocity of the acoustic branch, $\partial_\eta\lambda^a(\eta)$, is increasing on $[0,\pi/2]$, we conclude that $v = \partial_\eta\lambda^a(0) = 1$ and then the observability time of the numerical scheme is sharp: $T > 2$.* The following two auxiliary results hold:

PROPOSITION 6.2. *If the initial data $(\mathbf{U}_h^0, \mathbf{U}_h^1)$ in (2.2) belong to $(\mathcal{L}_h \times \mathcal{L}_h) \cap \mathcal{V}_h$, then the resonant Fourier coefficients in (3.22) vanish, i.e.*

$$\widehat{u}_\pm^r = 0 \tag{6.2}$$

*and the optic and the acoustic ones are related by the following two identities:*

$$\sum_{\alpha\in\{a,o\}} (\widehat{u}_+^{\alpha,k} + \widehat{u}_-^{\alpha,k}) \left( m^{\alpha,k} - n^{\alpha,k} \cos\left(\frac{k\pi h}{2}\right)\right) = 0 \tag{6.3}$$

*and*

$$\sum_{\alpha\in\{a,o\}} \lambda^{\alpha,k}(\widehat{u}_+^{\alpha,k} - \widehat{u}_-^{\alpha,k}) \left( m^{\alpha,k} - n^{\alpha,k} \cos\left(\frac{k\pi h}{2}\right)\right) = 0. \tag{6.4}$$

Taking squares in (6.3) and (6.4) and in view of (3.18), we deduce that

$$|\widehat{u}_+^{o,k} \pm \widehat{u}_-^{o,k}|^2 = f_\pm\Big(\frac{\Lambda^{a,k}}{\Lambda^{o,k}}\Big) \frac{W_1(\Lambda^{a,k})}{W_1(\Lambda^{o,k})} |\widehat{u}_+^{a,k} \pm \widehat{u}_-^{a,k}|^2, \tag{6.5}$$

where $f_+(x) = 1$, $f_-(x) = x$, for all $x \in \mathbb{R}$, and

$$W_1(\Lambda) = \frac{\Lambda^2(\Lambda^2 + 16\Lambda + 240)}{(\Lambda - 10)(19\Lambda^2 + 120\Lambda - 3600)}.$$

*Proof of Proposition 6.2.* We will prove only (6.2) and (6.3), the proof of (6.4) being similar to the one for (6.3). Observe that the Fourier representation of the identity that characterizes $\mathbf{U}_h^0 \in \mathcal{L}_h$ is

$$0 = \sum_{\alpha\in\{a,o\}}\sum_{k=1}^{N}(\widehat{u}_+^{\alpha,k}+\widehat{u}_-^{\alpha,k})\left(m^{\alpha,k}-n^{\alpha,k}\cos\left(\frac{k\pi h}{2}\right)\right)\sin(k\pi x_{j+1/2}) \tag{6.6}$$
$$+(\widehat{u}_+^{r}+\widehat{u}_-^{r})\frac{\sqrt{15}}{2\sqrt{2}}\sin((N+1)\pi x_{j+1/2}),$$

for all $j\in\mathbb{N}_N$. Multiplying (6.6) by $\sin(l\pi x_{j+1/2})$, $l\in\mathbb{N}_{N+1}^\star$, adding in $j\in\mathbb{N}_N$ and taking into account the orthogonality property below, we conclude the two identities (6.2) and (6.3):

$$h\sum_{j=0}^{N}\sin(k\pi x_{j+1/2})\sin(l\pi x_{j+1/2})=\frac{\delta_{k,l}}{2},\quad \forall k,l\in\mathbb{N}_{N+1}^\star. \qquad \square$$

The total energy of the data $(\mathbf{U}_h^0,\mathbf{U}_h^1)\in(\mathcal{L}_h\times\mathcal{L}_h)\cap\mathcal{V}_h$ in (2.2) can be written only in terms of the nodal components and coincides with the one of the $P_1$-finite element method

$$\mathcal{E}_h(\mathbf{U}_h^0,\mathbf{U}_h^1)=\frac{h}{2}\sum_{j=0}^{N}\left|\frac{U_{j+1}^0-U_j^0}{h}\right|^2+\frac{h}{12}\sum_{j=0}^{N}(2|U_j^1|^2+|U_{j+1}^1+U_j^1|^2). \tag{6.7}$$

Taking into account the form of the Fourier coefficients (6.2) and (6.5) corresponding to linear initial data, we obtain that the *Fourier representation* of the *total energy* (6.7) is as follows ($f_\pm$ being as in (6.5)):

$$\mathcal{E}_h(\mathbf{U}_h^0,\mathbf{U}_h^1)=\frac{1}{2}\sum_{k=1}^{N}\sum_{\pm}\Lambda_h^{a,k}\Big(1+f_\mp\Big(\frac{\Lambda^{o,k}}{\Lambda^{a,k}}\Big)\frac{W_1(\Lambda^{a,k})}{W_1(\Lambda^{o,k})}\Big)|\widehat{u}_+^{a,k}\pm\widehat{u}_-^{a,k}|^2. \tag{6.8}$$

The second auxiliary result establishes that for initial data in the bi-grid subspace $\mathcal{S}_h$ in (6.1), the high frequency Fourier coefficients on the acoustic branch can be evaluated in terms of the low frequency ones:

PROPOSITION 6.3. *For each element $(\mathbf{U}_h^0,\mathbf{U}_h^1)\in\mathcal{S}_h$ introduced in (6.1), the following identities hold:*

$$\widehat{u}_+^{a,(N+1)/2}=\widehat{u}_-^{a,(N+1)/2}=0, \tag{6.9}$$

$$\widehat{u}_+^{a,k'}+\widehat{u}_-^{a,k'}=-\frac{n^{a,k'}}{n^{a,k}}\frac{W_2(\Lambda^{a,k'})}{W_2(\Lambda^{a,k})}(\widehat{u}_+^{a,k}+\widehat{u}_-^{a,k}), \tag{6.10}$$

*with $k':=N+1-k$, and*

$$\widehat{u}_+^{a,k'}-\widehat{u}_-^{a,k'}=-\frac{n^{a,k'}}{n^{a,k}}\frac{W_2(\Lambda^{a,k'})}{W_2(\Lambda^{a,k})}\frac{\lambda^{a,k}}{\lambda^{a,k'}}(\widehat{u}_+^{a,k}-\widehat{u}_-^{a,k}), \tag{6.11}$$

*for all $k\in\mathbb{N}_{(N-1)/2}^\star$, with*

$$W_2(\Lambda)=\frac{(60-\Lambda)(\Lambda-10)(\Lambda-12)}{(\Lambda^2+16\Lambda+240)^2}.$$

Taking squares in (6.10-6.11), we obtain that

$$|\widehat{u}_+^{a,k'} + \widehat{u}_-^{a,k'}|^2 = \frac{W_3(\Lambda^{a,k'})}{W_3(\Lambda^{a,k})}|\widehat{u}_+^{a,k} + \widehat{u}_-^{a,k}|^2 \tag{6.12}$$

and

$$|\widehat{u}_+^{a,k'} - \widehat{u}_-^{a,k'}|^2 = \frac{\Lambda^{a,k}}{\Lambda^{a,k'}}\frac{W_3(\Lambda^{a,k'})}{W_3(\Lambda^{a,k})}|\widehat{u}_+^{a,k} - \widehat{u}_-^{a,k}|^2, \tag{6.13}$$

for all $k \in \mathbb{N}^\star_{(N-1)/2}$, where $W_3$ is as follows and $W_2$ is as in (6.11):

$$W_3(\Lambda) := W_2^2(\Lambda)\frac{(\Lambda-10)(\Lambda^2+16\Lambda+240)}{19\Lambda^2+120\Lambda-3600}.$$

*Proof of Proposition 6.3.* Due to the orthogonality in $\mathcal{H}_h^0$ of the eigenvectors in $\mathcal{EF}_h$, to the fact that $\mathbf{U}_h^0 \in \mathcal{L}_h$ and using the representation (3.18) of the normalized eigenvectors, the following identity holds:

$$\widehat{u}_+^{a,k} + \widehat{u}_-^{a,k} = (\mathbf{U}_h^0, \boldsymbol{\varphi}_h^{a,k})_{h,0} = \frac{4(60-\Lambda^{a,k})}{(\Lambda^{a,k})^2+16\Lambda^{a,k}+260}n^{a,k}h\sum_{j=1}^N U_j^0\sin(k\pi x_j). \tag{6.14}$$

Now, using the fact that $\mathbf{U}_h^0 \in \mathcal{B}_h$, we get

$$h\sum_{j=1}^N U_j^0\sin(k\pi x_j) = 2\cos^2\big(\frac{k\pi h}{2}\big)h\sum_{j=1}^{(N-1)/2} U_{2j}^0\sin(k\pi x_{2j}).$$

Taking (3.7) into account, we obtain

$$\widehat{u}_+^{a,k} + \widehat{u}_-^{a,k} = 16W_2(\Lambda^{a,k})n^{a,k}h\sum_{j=1}^{(N-1)/2} U_{2j}^0\sin(k\pi x_{2j}). \tag{6.15}$$

For $k=(N+1)/2$, we obtain $\widehat{u}_+^{a,(N+1)/2} + \widehat{u}_-^{a,(N+1)/2} = 0$. Since $\sin(k\pi x_{2j}) = -\sin(k'\pi x_{2j})$, by equating the expressions of $h\sum_{j=1}^{(N-1)/2} U_{2j}^0\sin(\widetilde{k}\pi x_{2j})$ from the identity (6.15) corresponding to $\widetilde{k} = k, k'$, we get (6.10). The proof of (6.11) is similar, based on the fact that $(\mathbf{U}_h^1, \boldsymbol{\varphi}_h^{a,k})_{h,0} = i\lambda_h^{a,k}(\widehat{u}_+^{a,k} - \widehat{u}_-^{a,k})$, from which, for $k=(N+1)/2$, we obtain $\widehat{u}_+^{a,(N+1)/2} - \widehat{u}_-^{a,(N+1)/2} = 0$, concluding (6.9). □

Replacing the Fourier representations (6.12) and (6.13) into the total energy with linear initial data (6.8), we obtain that energy corresponding to initial data $(\mathbf{U}_h^0, \mathbf{U}_h^1) \in \mathcal{S}_h$ in (6.1) is given by

$$\mathcal{E}_h(\mathbf{U}_h^0, \mathbf{U}_h^1) = \frac{1}{2}\sum_{k=1}^{(N-1)/2}\sum_{\pm}\Lambda_h^{a,k}(W_{\pm,k}^{lo} + W_{\pm,k}^{hi})|\widehat{u}_+^{a,k} \pm \widehat{u}_-^{a,k}|^2, \tag{6.16}$$

where the low and high frequency coefficients are given by ($f_\pm$ being as in (6.5))

$$W_{\pm,k}^{lo} := 1 + f_\mp\Big(\frac{\Lambda^{o,k}}{\Lambda^{a,k}}\Big)\frac{W_1(\Lambda^{a,k})}{W_1(\Lambda^{o,k})}, \quad W_{-,k}^{hi} := \left(1 + \frac{W_1(\Lambda^{a,k'})}{W_1(\Lambda^{o,k'})}\right)\frac{W_3(\Lambda^{a,k'})}{W_3(\Lambda^{a,k})},$$

with $k' := N + 1 - k$, and

$$W^{hi}_{+,k} := \frac{\Lambda^{a,k'}}{\Lambda^{a,k}} \left( 1 + \frac{\Lambda^{o,k'}}{\Lambda^{a,k'}} \frac{W_1(\Lambda^{a,k'})}{W_1(\Lambda^{o,k'})} \right) \frac{W_3(\Lambda^{a,k'})}{W_3(\Lambda^{a,k})}.$$

For any $\delta \in (0,1)$ which does not depend on $h$ and any solution (3.22) of (2.2), let us introduce its projection on the first $\lfloor \delta(N+1) \rfloor$ frequencies of the acoustic branch to be (here, $\lfloor \alpha \rfloor$ is the *integer part* of $\alpha \in \mathbb{R}$)

$$\Gamma^a_\delta \mathbf{U}_h(t) := \sum_{\pm} \sum_{k=1}^{\lfloor \delta(N+1) \rfloor} \widehat{u}^{a,k}_\pm \exp(\pm i t \lambda^{a,k}_h) \boldsymbol{\varphi}^{a,k}_h. \tag{6.17}$$

Observe that the projection (6.17) is still a solution of (2.2), therefore its total energy is conserved in time. Set

$$\mathcal{E}_h(\Gamma^a_\delta(\mathbf{U}^0_h, \mathbf{U}^1_h)) := \mathcal{E}_h(\Gamma^a_\delta \mathbf{U}_h(0), \Gamma^a_\delta \mathbf{U}_{h,t}(0)) = \sum_{k=1}^{\lfloor \delta(N+1) \rfloor} \Lambda^{a,k}_h (|\widehat{u}^{a,k}_+|^2 + |\widehat{u}^{a,k}_-|^2).$$

The following result provides an upper bound of the total energy of the solutions of (2.2) with initial data $(\mathbf{U}^0_h, \mathbf{U}^1_h) \in \mathcal{S}_h$ in (6.1) in terms of the total energy of their projections on the first half of the acoustic mode:

PROPOSITION 6.4. *For any solution $\mathbf{U}_h(t)$ of (2.2) with initial data $(\mathbf{U}^0_h, \mathbf{U}^1_h) \in \mathcal{S}_h$ in (6.1), there exists a constant $C > 0$ which does not depend on $h$ such that*

$$\mathcal{E}_h(\mathbf{U}^0_h, \mathbf{U}^1_h) \leq C \mathcal{E}_h(\Gamma^a_{1/2}(\mathbf{U}^0_h, \mathbf{U}^1_h)). \tag{6.18}$$

*Proof of Proposition 6.4.* In order to obtain the estimate (6.18), we claim that it is sufficient to prove that there exist $W^{lo}_\pm, W^{hi}_\pm > 0$ independent of $h$ such that $W^{lo}_{\pm,k} \leq W^{lo}_\pm$ and $W^{hi}_{\pm,k} \leq W^{hi}_\pm$, for all $1 \leq k \leq (N-1)/2$. Assuming this for a moment, we can take $C := \max\{W^{lo}_\pm, W^{hi}_\pm\}$, for which (6.18) holds.

Let us now analyze the boundedness of the four coefficients $W^{lo}_{\pm,k}$ and $W^{hi}_{\pm,k}$ in (6.16). Observe that $W^{lo}_{-,k}$ involves the product of $W_1(\Lambda^{a,k})$ and $1/W_1(\Lambda^{o,k})$ for $kh \leq 1/2$. But $W_1(\Lambda)$ is singular only for $\Lambda \to 10$, whereas for $kh \leq 1/2$, due to the increasing nature of $\Lambda^a$, we have $\Lambda^{a,k} \leq \Lambda^a(\pi/2) = 60/(13 + 2\sqrt{31}) < 3$. Also $1/W_1(\Lambda)$ is singular as $\Lambda \to 0$, but, since $\Lambda^o$ is decreasing in $\eta$, we get $\Lambda^{o,k} \geq \Lambda^o(\pi/2) = (52 + 8\sqrt{31})/3 > 30$ for all $kh \leq 1/2$. In the same way, $W^{lo}_{+,k}$ contains the product of $W_1(\Lambda^{a,k})/\Lambda^{a,k}$ with $\Lambda^{o,k}/W_1(\Lambda^{o,k})$, for $kh \leq 1/2$. The second factor, $\Lambda/W_1(\Lambda)$, has a singularity as $\Lambda \to 0$, but is evaluated for $\Lambda = \Lambda^{o,k}$ which is far from the singularity, for all $kh \leq 1/2$. Since $W_1(\Lambda)$ contains the factor $\Lambda^2$, we deduce that $W_1(\Lambda)/\Lambda$ has the same singularities as $W_1(\Lambda)$, i.e. $\Lambda = 10$, but since we work on the first half of the acoustic diagram, $\Lambda^{a,k}$ is far from that singularity. We conclude the existence of $W^{lo}_\pm > 0$ independent of $h$ such that $W^{lo}_{\pm,k} \leq W^{lo}_\pm$.

The coefficient $W^{hi}_{-,k}$ contains two terms. The first of them contains the factors $W_3(\Lambda^{a,k'})$ and $1/W_3(\Lambda^{a,k})$. Since $W_3(\Lambda)$ is not singular for any $\Lambda \in (0,10) \cup (12,60)$, then $W_3(\Lambda^{a,k'})$ is bounded for all $kh \leq 1/2$. On the other hand, $1/W_3(\Lambda)$ has three singularities: $\Lambda = 10$, $\Lambda = 12$ and $\Lambda = 60$. Since all $\Lambda$-s situated on the first half of the acoustic mode are far for all the three singularities, we deduce the boundedness of $1/W_3(\Lambda^{a,k})$. The second term is a product of four factors: $W_1(\Lambda^{a,k'})$, $W_3(\Lambda^{a,k'})$,

$1/W_1(\Lambda^{o,k'})$ and $1/W_3(\Lambda^{a,k})$. In view of our previous analysis, we deduce the boundedness of the last three factors. The first one blows-up like $1/(10-\Lambda^{a,k'})$ for small $k$. Nevertheless, in the same range of $k$-s, $W_3(\Lambda^{a,k'})$ behaves like $(10-\Lambda^{a,k'})^3$, compensating in this way the singularity of the first factor $W_1(\Lambda^{a,k'})$, so that $W_1(\Lambda^{a,k'})W_3(\Lambda^{a,k'})$ is bounded, for all $kh \leq 1/2$.

The coefficient $W^{hi}_{+,k}$ also contains two terms. The first of them includes the factors: $\Lambda^{a,k'}$, $1/\Lambda^{a,k}$, $W_3(\Lambda^{a,k'})$ and $1/W_3(\Lambda^{a,k})$. We have already analyzed the first, the third and the fourth ones. The second one blows-up like $\sin^{-2}(k\pi h/2)$ for small $k$. But, as we said, $W_3(\Lambda^{a,k'})$ behaves like $(10-\Lambda^{a,k'})^3 \sim \sin^6(k\pi h/2)$ for small $k$, compensating the singularity of the second factor, $1/\Lambda^{a,k}$. In this way, $W_3(\Lambda^{a,k'})/\Lambda^{a,k}$ is bounded, for all $kh \leq 1/2$. The second term in $W^{hi}_{+,k}$ contains the factors $1/\Lambda^{a,k}$, $\Lambda^{o,k'}$, $W_3(\Lambda^{a,k'})$ and $1/W_3(\Lambda^{a,k})$ and is bounded by the same arguments we used for the first term. Consequently, there exist $W^{hi}_{\pm} > 0$ such that $W^{hi}_{\pm,k} \leq W^{hi}_{\pm}$, which concludes the proof. □

*Remark 5. Set* $\mathcal{L}^\alpha_h := \{\mathbf{F}_h = (F_{j/2})_{j\in\mathbb{N}^\star_{2N+1}}$ *s.t.* $F_{j+1/2} = \alpha(F_j + F_{j+1}),\ j \in \mathbb{N}_N\}$ *and* $\mathcal{S}^\alpha_h := ((\mathcal{L}^\alpha_h \cap \mathcal{B}_h) \times (\mathcal{L}^\alpha_h \cap \mathcal{B}_h)) \cap \mathcal{V}_h$. *Observe that* $\mathcal{L}_h = \mathcal{L}^{1/2}_h$ *and* $\mathcal{S}_h = \mathcal{S}^{1/2}_h$, *where* $\mathcal{S}_h$ *is the space in (6.1). We want to point out that the result of Theorem 6.1 is not longer true when replace* $\mathcal{S}_h$ *by* $\mathcal{S}^\alpha_h$, *with* $\alpha \neq 1/2$, *so that the condition on the initial data to be linear is sharp. Indeed, when replacing* $\mathcal{S}_h$ *by* $\mathcal{S}^\alpha_h$, *in particular* $W^{lo}_{+,k}$ *in (6.16) has to be substituted by*

$$W^{lo,\alpha}_{+,k} := 1 + \frac{\Lambda^{o,k}}{\Lambda^{a,k}} \frac{W^\alpha_1(\Lambda^{a,k})}{W^\alpha_1(\Lambda^{o,k})}, \quad W^\alpha_1(\Lambda) = \frac{(\Lambda^2 + 16\Lambda + 240)(40 - 80\alpha + (1+8\alpha)\Lambda)^2}{25(\Lambda - 10)(19\Lambda^2 + 120\Lambda - 3600)}.$$

*One can show that, for* $\alpha \neq 1/2$, *it is not longer true that* $W^\alpha_1(\Lambda^{a,k}) \to 0$ *as* $kh \to 0$, *so that this factor cannot compensate the singularity of* $1/\Lambda^{a,k}$ *as* $kh \to 0$, *like for* $\alpha = 1/2$. *Consequently, for* $\alpha \neq 1/2$, *at least* $W^{lo,\alpha}_{+,k}$ *is not bounded for* $k \in \mathbb{N}^\star_{(N-1)/2}$.

*Proof of Theorem 6.1.* Proposition 6.3 ensures that the total energy of the initial data in $\mathcal{S}_h$ introduced in (6.1) is uniformly bounded by the energy of their projection on the first half of the acoustic mode. On the other hand, Theorem 5.1 guarantees that the observability inequality (2.6) with $B_h$ as in (2.7) holds uniformly as $h \to 0$ in the class of truncated data lying on the first half of the acoustic mode. Combining these two facts, one can apply a dyadic decomposition argument as in [16] and conclude the proof of Theorem 6.1. □

**6.2. The admissibility inequality.** In the rest of this section, our aim is to prove the direct inequality (2.8) for the boundary operator $B_h$ in (2.7) using the spectral identities (4.1) and (4.2). Firstly, let us observe that, for all matrix operators $B_h$ and all $T > 0$, we get the following inequalities:

$$\begin{aligned}\int_0^T ||B_h\mathbf{U}_h(t)||^2_{\mathbb{C}^{2N+1}}\,dt &= \int_0^T ((B_hS_h^{-1/2})^*B_hS_h^{-1/2}S_h^{1/2}\mathbf{U}_h(t), S_h^{1/2}\mathbf{U}_h(t))_{\mathbb{C}^{2N+1}}\,dt\\ &\leq ||(B_hS_h^{-1/2})^*B_hS_h^{-1/2}||_{\mathbb{C}^{2N+1}} \int_0^T (S_h\mathbf{U}_h(t), \mathbf{U}_h(t))_{\mathbb{C}^{2N+1}}\,dt\\ &\leq 2T\mathcal{E}_h(\mathbf{U}^0_h, \mathbf{U}^1_h)||(B_hS_h^{-1/2})^*B_hS_h^{-1/2}||_{\mathbb{C}^{2N+1}}. \qquad (6.19)\end{aligned}$$

For any matrix $A$, the matrix norm $||\cdot||_{\mathbb{C}^{2N+1}}$ involved in the right hand side of (6.19) is defined as

$$||A^*A||_{\mathbb{C}^{2N+1}} = \max_{||\boldsymbol{\varphi}_h||_{h,0}=1} ||AM_h^{1/2}\boldsymbol{\varphi}_h||_{\mathbb{C}^{2N+1}}.$$

In the above definition of the norm of a matrix, we can reduce the set of test functions to $\boldsymbol{\varphi}_h \in \mathcal{EF}_h$ introduced in (3.20), which is an orthonormal basis in $\mathbb{R}^{2N+1}$. Let us remark that for any eigenfunction $\boldsymbol{\varphi}_h \in \mathcal{EF}_h$, the corresponding eigenvalue $\Lambda_h \in \mathcal{EV}_h$ verifies the identity $S_h^{-1/2}M_h^{1/2}\boldsymbol{\varphi}_h = \Lambda_h^{-1/2}\boldsymbol{\varphi}_h$. Consequently, for any matrix $B_h$ and $\boldsymbol{\varphi}_h \in \mathcal{EF}_h$, the following identity holds:

$$||B_hS_h^{-1/2}M_h^{1/2}\boldsymbol{\varphi}_h||_{\mathbb{C}^{2N+1}} = \Lambda_h^{-1/2}||B_h\boldsymbol{\varphi}_h||_{\mathbb{C}^{2N+1}}. \tag{6.20}$$

Using (6.20), (4.1) and (4.2) for $B_h$ as in (2.7), we conclude that

$$||(B_hS_h^{-1/2})^*B_hS_h^{-1/2}||^2_{\mathbb{C}^{2N+1}} = \max_{\boldsymbol{\varphi}_h\in\mathcal{EF}_h} \frac{1}{\Lambda_h}\Big|\frac{\varphi_N}{h}\Big|^2 = \max\Big\{\max_{\Lambda\in(0,10)\cup(12,60)} W(\Lambda), \frac{3}{16}\Big\}$$

is independent of $h$.

**7. Convergence of the discrete controls.** In this section, we describe the algorithm of constructing the discrete controls of minimal $L^2(0,T)$-norm and we prove their convergence towards the continuous HUM boundary control $\tilde{v}(t)$ in (1.7) as $h \to 0$, under the hypothesis that both inverse and direct inequalities (2.6) and (2.8) hold uniformly as $h \to 0$. As we saw in the previous sections, the above hypothesis holds when the initial data in the adjoint system (2.2) is filtered through a Fourier truncation or a bi-grid algorithm.

**7.1. Description of the algorithm.** Using the *admissibility inequality* (2.8) and the *observability one* (2.6), one can prove the *continuity* and the *uniform coercivity* of $\mathcal{J}_h$ defined by (2.12) on $\mathcal{S}_h \subset \mathcal{V}_h$, where $\mathcal{S}_h$ can be both the truncated space (5.2) or the bi-grid one (6.1). Moreover, it is *strictly convex*. Applying the *direct method for the calculus of variations* (DMCV) (cf. [5]), one can guarantee the existence of an unique minimizer $(\tilde{\mathbf{U}}_h^0, \tilde{\mathbf{U}}_h^1)$ of $\mathcal{J}_h$, i.e.:

$$\mathcal{I}_h := \mathcal{J}_h(\tilde{\mathbf{U}}_h^0, \tilde{\mathbf{U}}_h^1) = \min_{(\mathbf{U}_h^0,\mathbf{U}_h^1)\in\mathcal{S}_h} \mathcal{J}_h(\mathbf{U}_h^0, \mathbf{U}_h^1). \tag{7.1}$$

Moreover, the Euler-Lagrange equation (2.13) associated to $\mathcal{J}_h$ characterizes the optimal control (2.14).

Remark that when the space of initial data in (2.2) is restricted to a subspace $\mathcal{S}_h \subset \mathcal{V}_h$, for example the ones given by (5.2) or (6.1), the exact controllability condition (2.10) holds for all $(\mathbf{U}_h^0, \mathbf{U}_h^1) \in \mathcal{S}_h$. This does not imply that the final state $(\mathbf{Y}_{h,t}(T), -\mathbf{Y}_h(T))$ in the controlled problem (2.9) is exactly controllable to the rest, but its orthogonal projection $\Gamma_{\mathcal{S}_h}$ from $\mathcal{V}_h$ on the subspace $\mathcal{S}_h$, i.e. $\Gamma_{\mathcal{S}_h}(\mathbf{Y}_{h,t}(T), -\mathbf{Y}_h(T)) = 0$, meaning that

$$\langle(\mathbf{Y}_{h,t}(T), -\mathbf{Y}_h(T)), (\mathbf{U}_h^0, \mathbf{U}_h^1)\rangle_{\mathcal{V}_h',\mathcal{V}_h} = 0,\ \forall(\mathbf{U}_h^0, \mathbf{U}_h^1) \in \mathcal{S}_h.$$

**7.2. The convergence result.** Set $\tilde{v}_h(t)$ to be the last component of the control $\tilde{\mathbf{V}}_h(t)$ in (2.14) (the other ones vanish). Since $\mathcal{I}_h \le \mathcal{J}_h(0,0) = 0$ and taking into account the inverse inequality (2.6), we obtain:

$$\int_0^T |\tilde{v}_h(t)|^2\,dt \le 8C(T)||(\mathbf{Y}_h^1, -\mathbf{Y}_h^0)||^2_{\mathcal{V}_h'}, \quad C(T) = \sup_{h\in(0,1)} C_h(T), \tag{7.2}$$

where $C_h(T)$ is the observability constant in (2.6) under filtering.

Set $\mathcal{EF} := \{\varphi^k(x) = \sqrt{2}\sin(k\pi x)\}$, $\Lambda^k := k^2\pi^2$, $\lambda^k := k\pi$ and $\ell^2$ be the space of square summable sequences. Since $\mathcal{EF}$ is a Hilbertian basis in each $H^s(0,1)$, $s \in \mathbb{R}$, the initial data $(y^1, -y^0) \in \mathcal{V}$ to be controlled in the continuous problem (1.1) admits the following Fourier decomposition:

$$y^i(x) = \sum_{k=1}^{\infty} \widehat{y}^{k,i}\varphi^k(x), \text{ with } \widehat{y}^{k,i} = (y^i, \varphi^k)_{L^2}, \ i = 0, 1. \tag{7.3}$$

Moreover, their $||\cdot||_{\mathcal{V}'}$-norm has the following Fourier representation:

$$||(y^1, -y^0)||^2_{\mathcal{V}'} = \sum_{k=1}^{\infty} \left( \frac{|\widehat{y}^{k,1}|^2}{\Lambda^k} + |\widehat{y}^{k,0}|^2 \right). \tag{7.4}$$

Since the set $\mathcal{EF}_h$ introduced in (3.20) is a basis in $\mathbb{R}^{2N+1}$, the initial data $(\mathbf{Y}^1_h, \mathbf{Y}^0_h) \in \mathcal{V}'_h$ to be controlled in the discrete problem (2.9) admit the following decomposition

$$\mathbf{Y}^i_h = \sum_{\alpha\in\{a,o\}} \sum_{k=1}^{N} \widehat{y}^{\alpha,k,i}_h \boldsymbol{\varphi}^{\alpha,k}_h + \widehat{y}^{r,i}_h \boldsymbol{\varphi}^r_h, \ \forall i = 0, 1, \tag{7.5}$$

with

$$\widehat{y}^{\alpha,k,i}_h = (\mathbf{Y}^i_h, \boldsymbol{\varphi}^{\alpha,k}_h)_{h,0}, \ \alpha \in \{a, o\}, 1 \le k \le N, \text{ and } \widehat{y}^{r,i}_h = (\mathbf{Y}^i_h, \boldsymbol{\varphi}^r_h)_{h,0}, \forall i = 0, 1.$$

Their $||\cdot||_{\mathcal{V}'_h}$-norm can be written in terms of the Fourier coefficients as follows:

$$||(\mathbf{Y}^1_h, -\mathbf{Y}^0_h)||^2_{\mathcal{V}'_h} = \sum_{k=1}^{N} \sum_{\alpha\in\{a,o\}} \frac{|\widehat{y}^{\alpha,k,1}_h|^2}{\Lambda^{\alpha,k}_h} + \frac{|\widehat{y}^{r,1}_h|^2}{\Lambda^r_h} + \sum_{k=1}^{N} \sum_{\alpha\in\{a,o\}} |\widehat{y}^{\alpha,k,0}_h|^2 + |\widehat{y}^{r,0}_h|^2. \tag{7.6}$$

The main result of this section is as follows:

THEOREM 7.1. *In the controlled problem (2.9), we consider initial data with the following two properties:*

$$\left( \frac{\widehat{y}^{a,k,1}_h}{\lambda^{a,k}_h} \right)_k \rightharpoonup \left( \frac{\widehat{y}^{k,1}}{\lambda^k} \right)_k, \quad (\widehat{y}^{a,k,0}_h)_k \rightharpoonup (\widehat{y}^{k,0})_k \text{ as } h \to 0, \text{ weakly in } \ell^2, \tag{7.7}$$

*and*

$$\left( \frac{\widehat{y}^{o,k,1}_h}{\lambda^{o,k}_h} \right)_k \rightharpoonup 0, \quad (\widehat{y}^{o,k,0}_h)_k \rightharpoonup 0 \text{ as } h \to 0, \text{ weakly in } \ell^2. \tag{7.8}$$

*Then*

$$\tilde{v}_h \rightharpoonup \tilde{v} \quad \text{as} \quad h \to 0, \quad \text{weakly in } L^2(0,T), \tag{7.9}$$

*where $\tilde{v}_h$ is the last component of the discrete optimal control $\tilde{\mathbf{V}}_h(t)$ given by (2.14) and obtained by the minimization of the functional $\mathcal{J}_h$ on the subspace $\mathcal{S}_h$ defined in (5.2) or in (6.1) and $\tilde{v}(t)$ is the continuous HUM control (1.7). Moreover, if the convergence in both (7.7) and (7.8) is strong, then the controls in (7.9) also converge strongly.*

The next result gives sufficient conditions for (7.7-7.8) to hold weakly/strongly:

PROPOSITION 7.2. *For all $y^0 \in L^2(0,1)$ and $y^1 \in H^{-1}(0,1)$, we define their projections on $\mathcal{U}_h$ to be*

$$y_h^i(x) := \sum_{k=1}^{N} \sum_{\alpha\in\{a,o\}} \widehat{y}_h^{\alpha,k,i}\varphi_h^{\alpha,k}(x) + \widehat{y}_h^{r,i}\varphi_h^r(x),\ i=0,1, \tag{7.10}$$

*where*

$$\widehat{y}_h^{\beta,0} = (y^0,\varphi_h^\beta)_{L^2} \text{ and } \widehat{y}_h^{\beta,1} = \langle y^1,\varphi_h^\beta\rangle_{H^{-1},H_0^1},\ \text{with } \beta=(\alpha,k) \text{ or } \beta=r. \tag{7.11}$$

*Then (7.7) and (7.8) hold. Moreover, $\widehat{y}_h^{r,0}$, $\widehat{y}_h^{r,1}/\lambda_h^r \to 0$ as $h\to 0$. For all $y^0 \in H_0^1(0,1)$ and $y^1\in L^2(0,1)$, we define their projections on $\mathcal{U}_h$ by (7.10), in which*

$$\widehat{y}_h^{\beta,0} = \frac{(y^0,\varphi_h^\beta)_{H_0^1}}{\Lambda_h^\beta} \text{ and } \widehat{y}_h^{\beta,1} = (y^1,\varphi_h^\beta)_{L^2},\ \text{with } \beta=(\alpha,k) \text{ or } \beta=r. \tag{7.12}$$

*Then (7.7) and 7.8) hold strongly as $h\to 0$.*

*Proof of Theorem 7.1.* Firstly, let us observe that from (7.7) and (7.8), we obtain that there exists a constant $C>0$ independent of $h$ such that

$$||(\mathbf{Y}_h^1, -\mathbf{Y}_h^0)||_{\mathcal{V}_h'} \le C. \tag{7.13}$$

By combining (7.2) and (7.13), we get the uniform boundedness as $h\to 0$ of the discrete control $\tilde{v}_h$ in $L^2(0,T)$, so that

$$\tilde{v}_h \rightharpoonup \tilde{v}^* \quad \text{as} \quad h\to 0, \quad \text{weakly in } L^2(0,T). \tag{7.14}$$

It is sufficient to prove that the weak limit $\tilde{v}^*$ coincides with the continuous HUM control $\tilde{v}$ given by (1.7).

The control $\tilde{v}$ can be characterized as the unique control $v$ in (1.1) which can be expressed as the space derivative of a solution of the adjoint problem (1.3) evaluated at $x=1$. Then, we have to prove that $\tilde{v}^*$ is an admissible control of the continuous wave equation, i.e. it verifies the identity (1.6), and that $\tilde{v}^* = \tilde{u}_x^*(1,t)$, where $\tilde{u}^*(x,t)$ is the solution of the adjoint problem (1.3) for some initial data $(\tilde{u}^{*,0},\tilde{u}^{*,1})\in\mathcal{V}$.

**Step I - The weak limit $\tilde{v}^*$ is a control in the continuous problem (1.1).** Since $\{(\pm\varphi^k/i\lambda^k,\varphi^k), k\in\mathbb{N}\}$ is an orthonormal basis in $\mathcal{V}:=H_0^1\times L^2(0,1)$, then the fact that $v$ is a control in (1.1), so it satisfies (1.6), is equivalent to prove (1.6) for all initial data of the form $(u^0,u^1)=(\pm\varphi^k/i\lambda^k,\varphi^k)$, $k\in\mathbb{N}$. The solution of the adjoint problem (1.3) with this kind of initial data is $u(x,t)=\pm\exp(\pm i\lambda^k(t-T))\varphi^k(x)/i\lambda^k$. Condition (1.6) is equivalent to the following one:

$$\int_0^T v(t)\exp(\pm it\lambda^k)\,dt = \frac{(-1)^k}{\sqrt{2}}\left(\frac{\widehat{y}^{k,1}}{\lambda^k} \mp i\widehat{y}^{k,0}\right), \forall k\in\mathbb{N}. \tag{7.15}$$

Let us check that $\tilde{v}^*$ satisfies (7.15). To do it, we distinguish between the two cases of subspaces $\mathcal{S}_h$ of filtered data. Firstly, let us consider the case of *Fourier truncated* initial data, i.e. $\mathcal{S}_h$ is given by (5.2). A particular class of initial data in $\mathcal{S}_h$ is $(\mathbf{U}_h^0,\mathbf{U}_h^1)=(\pm\boldsymbol{\varphi}_h^{a,k}/i\lambda_h^{a,k},\boldsymbol{\varphi}_h^{a,k})$, for which the solution of the discrete adjoint problem

(2.2) is $\mathbf{U}_h(t) = \pm\boldsymbol{\varphi}_h^{a,k}\exp(\pm i\lambda_h^{a,k}(t-T))/i\lambda_h^{a,k}$, for all $k\pi h \leq \eta_+^a$. From (2.13), we see that the discrete control $\tilde{v}_h$ verifies the identity

$$\int_0^T \tilde{v}_h(t)\exp(\pm it\lambda_h^{a,k})\,dt = \frac{(-1)^k}{n^{a,k}}\frac{\lambda_h^{a,k}}{\frac{\sin(k\pi h)}{h}}\left(\frac{\widehat{y}_h^{a,k,1}}{\lambda_h^{a,k}} \mp i\widehat{y}_h^{a,k,0}\right), \forall k\pi h \leq \eta_+^a. \quad (7.16)$$

Let us fix $k \in \mathbb{N}$ (independent of $h$). In that case, $\exp(\pm it\lambda_h^{a,k}) \to \exp(\pm it\lambda^k)$ as $h \to 0$ strongly in $L^2(0,T)$, so that, taking into account the weak convergence (7.14), we can pass to the limit as $h \to 0$ in the left hand side of (7.16) and we obtain the left hand side of (7.15) with $v$ substituted by $\tilde{v}^*$. On the other hand, taking into account the condition (7.7), which is valid for all test sequences in $\ell^2$ and in particular for the basis functions of $\ell^2$, $e^k = (0,\cdots,0,1,0,\cdots)$ (meaning that the weak convergence in $\ell^2$ is a pointwise convergence), and additionally the fact that $n^{a,k} \to \sqrt{2}$ and $\lambda_h^{a,k}/\sin(k\pi h)/h \to 1$ as $h \to 0$ for each fixed $k$, passing to the limit as $h \to 0$ in the right hand side of (2.13), we obtain the right hand side of (7.15). Then, the weak limit $\tilde{v}^*$ of the optimal control $\tilde{v}_h$ obtained by minimizing the functional $\mathcal{J}_h$ on $\mathcal{S}_h$ in (5.2) is a control for the continuous problem.

Let us consider now the case of linear data given by a *bi-grid algorithm*, i.e. $\mathcal{S}_h$ is as in (6.1). Taking into account Propositions 6.2 and 6.3, we see that, for initial data $(\mathbf{U}_h^0, \mathbf{U}_h^1) \in \mathcal{S}_h$, the Fourier representation (3.21) has the more particular form

$$\mathbf{U}_h^0 = \sum_{k=1}^{(N-1)/2}(\widehat{u}_+^{a,k} + \widehat{u}_-^{a,k})\psi_h^k \text{ and } \mathbf{U}_h^1 = \sum_{k=1}^{(N-1)/2}(\widehat{u}_+^{a,k} - \widehat{u}_-^{a,k})i\lambda_h^{a,k}\psi_h^k. \quad (7.17)$$

The basis function $\psi_h^k$ generating $\mathcal{S}_h$ has the explicit form below (with $k' := N+1-k$):

$$\psi_h^k = \boldsymbol{\varphi}_h^{a,k} - \frac{W_4(\Lambda^{a,k})}{W_4(\Lambda^{o,k})}\boldsymbol{\varphi}_h^{o,k} - \frac{W_5(\Lambda^{a,k'})}{W_5(\Lambda^{a,k})}\boldsymbol{\varphi}_h^{a,k'} + \frac{W_5(\Lambda^{a,k'})}{W_5(\Lambda^{a,k})}\frac{W_4(\Lambda^{a,k'})}{W_4(\Lambda^{o,k'})}\boldsymbol{\varphi}_h^{o,k'}, \quad (7.18)$$

where

$$W_4(\Lambda) = -\frac{\Lambda}{\Lambda-10}\sqrt{\tilde{W}(\Lambda)} \text{ and } W_5(\Lambda) = \frac{(60-\Lambda)(\Lambda-10)(\Lambda-12)}{(\Lambda^2+16\Lambda+240)^2}\sqrt{\tilde{W}(\Lambda)}$$

and $\tilde{W}$ as in (3.17). Let us fix $k \in \mathbb{N}^\star_{(N-1)/2}$ and consider the homogeneous problem (2.2) with initial data $(\mathbf{U}_h^0, \mathbf{U}_h^1) = (s\psi^k/i\lambda_h^{a,k}, \psi^k)$, $s \in \{-1,+1\}$, for which the solution takes the form

$$\mathbf{U}_h(t) = \sum_{\alpha\in\{a,o\}}\big(\widehat{u}_{lo}^{\alpha,k}(t)\boldsymbol{\varphi}_h^{\alpha,k} + \widehat{u}_{hi}^{\alpha,k}(t)\boldsymbol{\varphi}_h^{\alpha,N+1-k}\big), \quad (7.19)$$

where the low frequency coefficients are $\widehat{u}_{lo}^{a,k}(t) := s\exp(is\lambda_h^{a,k}(t-T))/(i\lambda_h^{a,k})$ and

$$\widehat{u}_{lo}^{o,k}(t) := -\frac{W_4(\Lambda^{a,k})}{W_4(\Lambda^{o,k})}\sum_{\pm}\frac{1}{2}\Big(\frac{s}{i\lambda_h^{a,k}} \pm \frac{1}{\lambda_h^{o,k}}\Big)\exp(\pm i\lambda_h^{o,k}(t-T)),$$

while the high frequency ones are as follows (with $k' := N+1-k$):

$$\widehat{u}_{hi}^{a,k}(t) := -\frac{W_5(\Lambda^{a,k'})}{W_5(\Lambda^{a,k})}\sum_{\pm}\frac{1}{2}\Big(\frac{s}{i\lambda_h^{a,k}} \pm \frac{1}{\lambda_h^{a,k'}}\Big)\exp(\pm i\lambda_h^{a,k'}(t-T))$$

and

$$\widehat{u}_{hi}^{o,k}(t) := \frac{W_5(\Lambda^{a,k'})}{W_5(\Lambda^{a,k})}\frac{W_4(\Lambda^{a,k'})}{W_4(\Lambda^{o,k'})}\sum_{\pm}\frac{1}{2}\Big(\frac{s}{i\lambda_h^{a,k}}\pm\frac{1}{\lambda_h^{o,k'}}\Big)\exp(\pm i\lambda_h^{o,k'}(t-T)).$$

By considering the particular class of solutions given by (7.19) into (2.13), we see that the control $\tilde{v}_h(t)$ satisfies the identity

$$\int_0^T \tilde{v}_h(t)\exp(is\lambda_h^{a,k}t)\,dt = \frac{(-1)^k}{n^{a,k}}\frac{h\lambda_h^{a,k}}{\sin(k\pi h)}\left(\frac{\widehat{y}_h^{a,k,1}}{\lambda_h^{a,k}} - is\widehat{y}_h^{a,k,0}\right) + \frac{is(-1)^k}{n^{a,k}}\frac{h\lambda_h^{a,k}}{\sin(k\pi h)}(E_{h,1}^k+E_{h,2}^k)\exp(is\lambda_h^{a,k}T), \tag{7.20}$$

where the error terms are as follows (with $k' := N+1-k$)

$$E_{h,1}^k = -(-1)^k\frac{\sin(k\pi h)}{h}\int_0^T \tilde{v}_h(t)\big(\widehat{u}_{lo}^{o,k}(t)n^{o,k} + \sum_{\alpha\in\{a,o\}}\widehat{u}_{hi}^{\alpha,k}(t)n^{\alpha,k'}\big)\,dt$$

and

$$E_{h,2}^k = \widehat{y}_{h,1}^{o,k}\widehat{u}_{lo}^{o,k}(0) + \sum_{\alpha\in\{a,o\}}\widehat{y}_{h,1}^{\alpha,k'}\widehat{u}_{hi}^{\alpha,k}(0) - \widehat{y}_{h,0}^{o,k}\widehat{u}_{lo,t}^{o,k}(0) - \sum_{\alpha\in\{a,o\}}\widehat{y}_{h,0}^{\alpha,k'}\widehat{u}_{hi,t}^{\alpha,k}(0).$$

Passing to the limit as $h\to 0$ in the left hand side and in the first term in the right hand side of (7.20) can be done as for the truncated space $\mathcal{S}_h$ in (5.2). Therefore, in order to prove that the weak limit $\tilde{v}^*$ satisfies (7.15), it is enough to show that the error terms are small as $h\to 0$, i.e.

$$|E_{h,1}^k|\to 0 \text{ and } |E_{h,2}^k|\to 0 \text{ as } h\to 0. \tag{7.21}$$

From the fact that the $L^2(0,T)$-norm of the discrete control $\tilde{v}_h(t)$ is uniformly bounded as $h\to 0$, the Cauchy-Schwartz inequality and the explicit expressions of $\widehat{u}_{lo}^{o,k}(t)$, $\widehat{u}_{hi}^{a,k}(t)$ and $\widehat{u}_{hi}^{o,k}(t)$, we obtain

$$|E_{h,1}^k| \le C\sqrt{T}\big(E_{h,1}^{k,1}+E_{h,1}^{k,2}+E_{h,1}^{k,3}\big)^{1/2},$$

where

$$E_{h,1}^{k,1} := |n^{o,k}|^2\Big|\frac{W_4(\Lambda^{a,k})}{W_4(\Lambda^{o,k})}\Big|^2\Big(\frac{\sin^2(k\pi h)}{\Lambda^{a,k}}+\frac{\sin^2(k\pi h)}{\Lambda^{o,k}}\Big),$$

$$E_{h,1}^{k,2} := |n^{a,k'}|^2\Big|\frac{W_5(\Lambda^{a,k'})}{W_5(\Lambda^{a,k})}\Big|^2\Big(\frac{\sin^2(k\pi h)}{\Lambda^{a,k}}+\frac{\sin^2(k\pi h)}{\Lambda^{a,k'}}\Big),$$

$$E_{h,1}^{k,3} := |n^{o,k'}|^2\Big|\frac{W_4(\Lambda^{a,k'})}{W_4(\Lambda^{o,k'})}\Big|^2\Big|\frac{W_5(\Lambda^{a,k'})}{W_5(\Lambda^{a,k})}\Big|^2\Big(\frac{\sin^2(k\pi h)}{\Lambda^{a,k}}+\frac{\sin^2(k\pi h)}{\Lambda^{o,k'}}\Big),$$

$k' := N+1-k$ and $W_4$, $W_5$ are as in (7.18).

On the other hand, since the $||\cdot||_{\mathcal{V}_h'}$ - norm of the initial data $(\mathbf{Y}_h^1, \mathbf{Y}_h^0)$ to be controlled is uniformly bounded as $h \to 0$, we see that

$$|E_{h,2}^k| \leq C(E_{h,2}^{k,1} + E_{h,2}^{k,2} + E_{h,2}^{k,3})^{1/2},$$

with

$$E_{h,2}^{k,1} := \Lambda_h^{o,k}|\widehat{u}_{lo}^{o,k}(0)|^2 + |\widehat{u}_{lo,t}^{o,k}(0)|^2 = \Big|\frac{W_4(\Lambda^{a,k})}{W_4(\Lambda^{o,k})}\Big|^2\Big(\frac{\Lambda^{o,k}}{\Lambda^{a,k}} + 1\Big),$$

$$E_{h,2}^{k,2} := \Lambda_h^{a,k'}|\widehat{u}_{hi}^{a,k}(0)|^2 + |\widehat{u}_{hi,t}^{a,k}(0)|^2 = \Big|\frac{W_5(\Lambda^{a,k'})}{W_5(\Lambda^{a,k})}\Big|^2\Big(\frac{\Lambda^{a,k'}}{\Lambda^{a,k}} + 1\Big),$$

$k' := N + 1 - k$ and

$$E_{h,2}^{k,3} := \Lambda_h^{o,k'}|\widehat{u}_{hi}^{o,k}(0)|^2 + |\widehat{u}_{hi,t}^{o,k}(0)|^2 = \Big|\frac{W_4(\Lambda^{a,k'})}{W_4(\Lambda^{o,k'})}\Big|^2\Big|\frac{W_5(\Lambda^{a,k'})}{W_5(\Lambda^{a,k})}\Big|^2\Big(\frac{\Lambda^{o,k'}}{\Lambda^{a,k}} + 1\Big).$$

For a fixed $k \in \mathbb{N}$, let us study the limit as $h \to 0$ of $E_{h,j}^{k,i}$, for $1 \leq i \leq 3$, $1 \leq j \leq 2$:

- From $|n^{o,k}|^2 \to 3\tilde{W}(60) = 10$ ($\tilde{W}$ introduced in (3.17)), $|W_4(\Lambda^{a,k})|^2 \to |W_4(0)|^2 = 0$, $|W_4(\Lambda^{o,k})|^2 \to |W_4(60)|^2 = 24/25$, $\sin^2(k\pi h)/\Lambda^{a,k} \to 1$ and $\sin^2(k\pi h)/\Lambda^{o,k} \to 0$, we see that $E_{h,1}^{k,1} \to 0$ as $h \to 0$.
- From $|n^{a,k'}|^2 \to 3\tilde{W}(10) = 0$, $|W_5(\Lambda^{a,k'})|^2 \to |W_5(10)|^2 = 0$, $|W_5(\Lambda^{a,k})|^2 \to |W_5(0)|^2 = 1/96$ and $\sin^2(k\pi h)/\Lambda^{a,k'} \to 0$, we see that $E_{h,1}^{k,2} \to 0$ as $h \to 0$.
- Remark that $|n^{o,k'}|^2 \to 3\tilde{W}(12) = 6$, $|W_4(\Lambda^{o,k'})|^2 \to |W_4(12)|^2 = 72$ and $\sin^2(k\pi h)/\Lambda^{o,k'} \to 0$, but $|W_4(\Lambda^{a,k'})|^2 \to |W_4(10)|^2 = \infty$. Nevertheless, $|W_4(\Lambda^{a,k'})|^2|W_5(\Lambda^{a,k'})|^2 \to 0$, so that, at the end, $E_{h,1}^{k,3} \to 0$ as $h \to 0$.
- Remark that $\Lambda^{o,k} \to 60$ and $\Lambda^{a,k} \to 0$. Moreover, $|W_4(\Lambda^{a,k})|^2 \to 0$ like $|\Lambda^{a,k}|^2$. This compensates the singularity of $1/\Lambda^{a,k}$, so that $E_{h,2}^{k,1} \to 0$ as $h \to 0$.
- $|W_5(\Lambda^{a,k'})|^2 \to 0$ since it involves the factor $(10-\Lambda^{a,k'})^3 \sim \sin^6(k\pi h/2)$. This cancels the singularity introduced by $1/\Lambda^{a,k} \sim 1/\sin^2(k\pi h/2)$ and ensures that $E_{h,2}^{k,2} \to 0$ as $h \to 0$.
- $|W_4(\Lambda^{a,k'})|^2|W_5(\Lambda^{a,k'})|^2 \to 0$ since it contains the factor $(10 - \Lambda^{a,k'})^2 \sim \sin^4(k\pi h/2)$, which compensates the singularity of $1/\Lambda^{a,k} \sim 1/\sin^2(k\pi h/2)$ so that $E_{h,2}^{k,3} \to 0$ as $h \to 0$.

This concludes (7.21) and the fact that the weak limit $\tilde{v}^*$ of the sequence of discrete HUM controls obtained by minimizing the functional $\mathcal{J}_h$ over the bi-grid class $\mathcal{S}_h$ in (6.1) is a control in the continuous problem (1.1).

**Step II - The weak limit $\tilde{v}^*$ is the normal derivative of a solution of the continuous adjoint problem (1.3).** Consider $(\tilde{\mathbf{U}}_h^0, \tilde{\mathbf{U}}_h^1) \in \mathcal{S}_h$ (which in what follows can be both the subspace in (5.2) or the one in (6.1)) to be the minimum of the functional $\mathcal{J}_h$. Due to the uniform nature of the observability inequality (2.6), $\mathcal{E}_h(\tilde{\mathbf{U}}_h^0, \tilde{\mathbf{U}}_h^1)$ is uniformly bounded, i.e. there exists $C > 0$ independent of $h$ such that

$$\mathcal{E}_h(\tilde{\mathbf{U}}_h^0, \tilde{\mathbf{U}}_h^1) = \frac{1}{2}\sum_{k=1}^{N}\sum_{\alpha\in\{a,o\}}(\Lambda_h^{\alpha,k}|\widehat{\tilde{u}}_h^{\alpha,k,0}|^2 + |\widehat{\tilde{u}}_h^{\alpha,k,1}|^2) \leq C. \tag{7.22}$$

Due to the property (6.2), the resonant mode in the solution of the adjoint problem (2.2) for initial data in the filtered space $\mathcal{S}_h$ in (5.2) or in (6.1) vanishes, so that the Fourier representation of the total energy in the left hand side of (7.22) is valid for both filtered spaces $\mathcal{S}_h$ in (5.2) and (6.1).

Remark however that the high frequency components vanish for data in the truncation subspace $\mathcal{S}_h$ in (5.2). On the other hand, for data in the bi-grid space $\mathcal{S}_h$ in (6.1), the relations between the optic and the acoustic modes and the high frequencies in the acoustic mode and the lowest ones described in Propositions 6.2 and 6.3 hold.

From (7.22), we deduce the following weak limits as $h \to 0$ in $\ell^2$:

$$(\lambda_h^{a,k}\widehat{\widetilde{u}}_h^{a,k,0})_k \rightharpoonup (\lambda^k \widehat{\widetilde{u}}^{*,k,0})_k,\ (\widehat{\widetilde{u}}_h^{a,k,1})_k \rightharpoonup (\widehat{\widetilde{u}}^{*,k,1})_k, \quad \Big(\frac{\widehat{\widetilde{u}}_h^{o,k,1}}{\lambda_h^{o,k}}\Big)_k,\ (\widehat{\widetilde{u}}_h^{o,k,0})_k \rightharpoonup 0. \tag{7.23}$$

Set $\tilde{u}^{*,i}(x) := \sum_{k=1}^{\infty} \widehat{\widetilde{u}}^{*,k,i}\varphi^k(x)$. Remark that $(\tilde{u}^{*,0}, \tilde{u}^{*,1}) \in \mathcal{V}$ and denote by $\tilde{u}^*(x,t)$ the corresponding solution of (1.3). Firstly, we prove that

$$-\frac{\tilde{U}_N(t)}{h} \rightharpoonup \tilde{u}_x^*(1,t) \text{ as } h \to 0 \text{ weakly in } L^2(0,T). \tag{7.24}$$

In fact, for arbitrary functions $\psi \in L^2(0,T)$ and $\psi_\epsilon \in C_0^k(0,T)$, we will prove the following estimate:

$$\Big|\int_0^T \Big(-\frac{\tilde{U}_N(t)}{h} - \tilde{u}_x^*(1,t)\Big)\psi(t)\,dt\Big| \le \Big|\int_0^T \Big(-\frac{\Gamma^a\tilde{U}_N(t)}{h} - \tilde{u}_x^*(1,t)\Big)\psi(t)\,dt\Big| + C||\psi-\psi_\epsilon||_{L^2(0,T)} + Ch^k||\psi_\epsilon^{(k)}||_{L^2(0,T)}, \tag{7.25}$$

where $\Gamma^a := \Gamma_1^a$ is the projection on the acoustic branch defined by (6.17). In a similar way, we define the projection on the optic branch, $\Gamma^o$. In order to prove (7.25), we decompose its right hand side as follows:

$$\int_0^T \Big(-\frac{\tilde{U}_N(t)}{h} - \tilde{u}_x^*(1,t)\Big)\psi(t)\,dt = \int_0^T \Big(-\frac{\Gamma^a\tilde{U}_N(t)}{h} - \tilde{u}_x^*(1,t)\Big)\psi(t)\,dt + \int_0^T \Big(-\frac{\Gamma^o\tilde{U}_N(t)}{h}\Big)(\psi(t)-\psi_\epsilon(t))\,dt + \int_0^T \Big(-\frac{\Gamma^o\tilde{U}_N(t)}{h}\Big)\psi_\epsilon(t)\,dt =: I_h^1 + I_h^2 + I_h^3.$$

Taking into account that $\psi_\epsilon \in C_c^k(0,T)$, by integration by parts, we get

$$I_h^3 = (-1)^k \int_0^T \psi_\epsilon^{(k)}(t)\Big(\sum_{\pm}\sum_{l=1}^N \widehat{\widetilde{u}}_\pm^{o,l}\frac{1}{(\pm i\lambda_h^{o,l})^k}\exp(\pm i\lambda_h^{o,l}(t-T))\Big(-\frac{\varphi_N^{o,l}}{h}\Big)\Big)\,dt.$$

From the Cauchy-Schwartz and the admissibility inequality, the bound (7.22) and the fact that $\Lambda_h^{o,l} \ge 12/h^2$ for all $l \in \mathbb{N}_N^\star$, we deduce that

$$|I_h^2| \le \Big|\Big|-\frac{\Gamma^o\tilde{U}_N}{h}\Big|\Big|_{L^2(0,T)}||\psi-\psi_\epsilon||_{L^2(0,T)} \lesssim ||\psi-\psi_\epsilon||_{L^2(0,T)}\Big(\sum_{l=1}^N \Lambda_h^{o,l}(|\widehat{\widetilde{u}}_+^{o,l}|^2 + |\widehat{\widetilde{u}}_-^{o,l}|^2)\Big)^{1/2} \lesssim ||\psi-\psi_\epsilon||_{L^2(0,T)}$$

and

$$|I_h^3| \leq ||\psi_\epsilon^{(k)}||_{L^2(0,T)} \Big|\Big| \sum_{\pm} \sum_{l=1}^{N} \widehat{\tilde{u}}_{\pm}^{o,l} \frac{1}{(\pm i\lambda_h^{o,l})^k} \exp(\pm i\lambda_h^{o,l}(\cdot - T)) \Big( - \frac{\varphi_N^{o,l}}{h} \Big) \Big|\Big|_{L^2(0,T)}$$

$$\lesssim ||\psi_\epsilon^{(k)}||_{L^2(0,T)} \Big( \sum_{l=1}^{N} \Lambda_h^{o,l} (|\widehat{\tilde{u}}_+^{o,l}|^2 + |\widehat{\tilde{u}}_-^{o,l}|^2)(\Lambda_h^{o,l})^{-k} \Big)^{1/2} \lesssim h^k ||\psi_\epsilon^{(k)}||_{L^2(0,T)}.$$

Once we get (7.25), we conclude (7.24) by using the following three ingredients: i) the weak convergence (7.7) combined with the strong convergence $n^{a,l} \to \sqrt{2}$, $\sin(l\pi h)/\lambda^{a,l} \to 1$ and

$$\int_0^T \psi(t) \exp(\pm i(t-T)\lambda_h^{a,l})\, dt \to \int_0^T \psi(t) \exp(\pm i(t-T)\lambda^l)\, dt \text{ as } h \to 0,$$

allowing us to pass to the limit as $h \to 0$ in $I_h := \int_0^T (-\Gamma^a \tilde{U}_N(t)/h)\psi(t)\, dt$ or, equivalently, in the sense of $\ell^2$ in each term on the right hand side of

$$I_h = \sum_{\pm} \sum_{l=1}^{N} \lambda_h^{a,l} \widehat{\tilde{u}}_{\pm}^{a,l} n^{a,l} (-1)^l \frac{\sin(l\pi h)}{\lambda^{a,l}} \int_0^T \psi(t) \exp(\pm i(t-T)\lambda_h^{a,l})\, dt,$$

so that we can guarantee that the first term $I_h^1$ in the right hand side of (7.25) is small as $h \to 0$; ii) the density of $C_c^k(0,T)$ in $L^2(0,T)$, allowing to choose $\epsilon$ so that $||\psi - \psi_\epsilon||_{L^2(0,T)}$ is arbitrarily small; iii) an appropriate choice of the mesh size $h$ according to $\epsilon$, so that $h^k ||\psi_\epsilon^{(k)}||_{L^2(0,T)}$ is arbitrarily small.

Let us check that $\tilde{v}^* = \tilde{u}_x^*(1,t)$ in $L^2(0,T)$. Indeed, using (7.14), (7.24), we get:

$$\int_0^T \tilde{v}^*(t)\psi(t)\, dt = \lim_{h\to 0} \int_0^T \tilde{v}_h(t)\psi(t)\, dt = \lim_{h\to 0} \int_0^T \Big( - \frac{\tilde{U}_N(t)}{h} \Big) \psi(t)\, dt = \int_0^T \tilde{u}_x^*(1,t)\psi(t)\, dt,$$

for any $\psi \in L^2(0,T)$. Therefore, $\tilde{v}^* = \tilde{v}$ in $L^2(0,T)$ and also $\tilde{u}_x^*(1,t) = \tilde{u}_x(1,t)$, which, jointly with the continuous observability inequality (1.4) yields $(\tilde{u}^{*,0}, \tilde{u}^{*,1}) = (\tilde{u}^0, \tilde{u}^1)$ in $\mathcal{V}$ and then $(\widehat{\tilde{u}}^{*,k,i})_k = (\widehat{\tilde{u}}^{k,i})_k$ in $\ell^2$, $i = 0, 1$. Consequently, once we have identified that the weak limit of the discrete controls is the continuous HUM control, we get the $\Gamma$-convergence of the discrete minimizer to the continuous one.

**Step III - Strong convergence of the discrete controls.** In order to prove that $\tilde{v}_h$ converges strongly in $L^2(0,T)$ to $\tilde{v}$ as $h \to 0$, it is enough to prove that

$$\lim_{h\to 0} \int_0^T |\tilde{v}_h(t)|^2\, dt = \int_0^T |\tilde{v}(t)|^2\, dt. \tag{7.26}$$

Using as test function $\mathbf{U}_h(t)$ in (2.13) the solution $\tilde{\mathbf{U}}_h(t)$ of (2.2) corresponding to the minimizer $(\widetilde{\mathbf{U}}_h^0, \widetilde{\mathbf{U}}_h^1) \in \mathcal{S}_h$ of $\mathcal{J}_h$ in (2.12), we get

$$\int_0^T \Big| \frac{\tilde{U}_N(t)}{h} \Big|^2 dt = \langle (\mathbf{Y}_h^1, -\mathbf{Y}_h^0), (\tilde{\mathbf{U}}_h(0), \tilde{\mathbf{U}}_{h,t}(0)) \rangle_{\mathcal{V}_h', \mathcal{V}_h} = \sum_{\alpha \in \{a,o\}} P_h^\alpha \tag{7.27}$$

and, additionally, $||\tilde{v}_h||^2_{L^2(0,T)} = ||\tilde{U}_N/h||^2_{L^2(0,T)}$ (from 2.14). Here,

$$P_h^\alpha = \sum_{\pm}\sum_{k=1}^{N} \frac{1}{2}\Big(\frac{\widehat{y}_h^{\alpha,k,1}}{i\lambda_h^{\alpha,k}} \mp \widehat{y}_h^{\alpha,k,0}\Big)\big(i\lambda_h^{\alpha,k}\widehat{\tilde{u}}_h^{\alpha,k,0} \pm \widehat{\tilde{u}}_h^{\alpha,k,1}\big)\exp(\mp iT\lambda_h^{\alpha,k}).$$

Let us remark that using the strong convergence of the acoustic part of the initial data to be controlled (7.7) and the boundedness of the energy of the minimizer of $\mathcal{J}_h$,

$$\lim_{h\to 0} P_h^a = \sum_{\pm}\sum_{k=1}^{\infty} \frac{1}{2}\Big(\frac{\widehat{y}^{k,1}}{i\lambda^k} \mp \widehat{y}^{k,0}\Big)\big(i\lambda^k\widehat{\tilde{u}}^{k,0} \pm \widehat{\tilde{u}}^{k,1}\big)\exp(\mp iT\lambda^k) = \int_0^T |\tilde{u}_x(1,t)|^2\,dt.$$

Additionally, $||\tilde{v}||^2_{L^2(0,T)} = ||\widetilde{u}_x(1,\cdot)||^2_{L^2(0,T)}$ (from (1.7)). On the other hand, from the uniform boundedness of the energy of the minimizer of $\mathcal{J}_h$, we get

$$|P_h^o|^2 \le C\sum_{k=1}^{N}\Big(\frac{|\widehat{y}_h^{o,k,1}|^2}{\Lambda_h^{o,k}} + |\widehat{y}_h^{o,k,0}|^2\Big) \to 0 \text{ as } h\to 0,$$

which concludes (7.26) and the strong convergence of the optimal control. □

*Proof of Proposition 7.2.* Consider firstly $y^0 \in L^2(0,1)$, so that $y^0(x) = \sum_{k\ge 1}\widehat{y}^{k,0}\varphi^k(x)$, with $||y^0||^2_{L^2} = \sum_{k\ge 1}|\widehat{y}^{k,0}|^2 < \infty$. Take $y_h^0 \in \mathcal{U}_h$ of Fourier coefficients given by (7.11). The discrete data $y_h^0$ constructed in this way is the $L^2(0,1)$-projection of $y^0$ on $\mathcal{U}_h$, in the sense that $(y^0 - y_h^0, \phi_h)_{L^2} = 0$ and $||y^0 - y_h^0||_{L^2} \le ||y^0 - \phi_h||_{L^2}$, for all $\phi_h \in \mathcal{U}_h$. Clearly, $||y_h^0||_{L^2} \le ||y^0||_{L^2}$, so that, in order to obtain the second weak convergence in both (7.7) and (7.8), it is sufficient to fix $k \in \mathbb{N}$ and to show that $\widehat{y}_h^{a,k,0} \to \widehat{y}^{k,0}$ and that $\widehat{y}_h^{o,k,0} \to 0$ as $h \to 0$. Using the explicit form (3.12) and (3.17) of the eigenvectors and (3.19), we can easily compute $\widehat{y}_h^{\alpha,k,0}$ and $\widehat{y}_h^{r,0}$ as follows:

$$\widehat{y}_h^{\alpha,k,0} = \widehat{y}^{k,0}\left(2\sin^2\Big(\frac{k\pi h}{2}\Big) + \frac{5\Lambda^{\alpha,k}\beta_h^k}{10-\Lambda^{\alpha,k}}\right)\frac{\sqrt{6\widetilde{W}(\Lambda^{\alpha,k})}}{(k\pi h)^2} + r_h^{\alpha,k,0}, \tag{7.28}$$

with $\beta_h^k := \sin^2(k\pi h/2) + \sin(k\pi h)/(k\pi h) - 1$, and

$$\widehat{y}_h^{r,0} = \sum_{l=1}^{\infty}\widehat{y}^{(2l-1)(N+1),0}\frac{8\sqrt{15}}{(2l-1)^3\pi^3}. \tag{7.29}$$

The term $r_h^{\alpha,k,0}$ is of the form $\sum_{m=1}^{\infty}\widehat{y}^{2m(N+1)\pm k,0}\beta_m$, with $(\beta_m)_{m\in\mathbb{N}} \in \ell^2$. It converges to zero due to the fact that it has an upper bound in terms of the reminder of order $N+1$ of the series $\sum_{k\in\mathbb{N}}|\widehat{y}^{k,0}|^2$. The convergence $\widehat{y}_h^{a,k,0} \to \widehat{y}^{k,0}$ holds since $\Lambda^{a,k}/(k\pi h)^2 \to 1$ and $\sqrt{6\tilde{W}(\Lambda^{a,k})} \to 2$ as $h \to 0$. Since $\Lambda^{o,k} \to 60$, $2\sin(k\pi h/2)/(k\pi h) \to 1$, $(\sin(k\pi h)/(k\pi h) - 1)/(k\pi h)^2 \to -1/6$ and $\sqrt{6\tilde{W}(\Lambda^{a,k})} \to \sqrt{20}$, we conclude that $\widehat{y}_h^{o,k,0} \to 0$ as $h \to 0$. The coefficient of the resonant mode, $\widehat{y}_h^{r,0}$, tends to zero as $h \to 0$ due to the fact that (7.29) can be bounded from above by the reminder of order $N+1$ of a convergent series. One could intuit the last convergence in (7.7) since, for a fixed $k \in \mathbb{N}$, $\varphi_h^{a,k} \to \varphi^k$ in $L^2(0,1)$. In $\varphi_h^{o,k}$, the vector of nodal components behaves like $\sqrt{5}\varphi^k$, while the one of the midpoints components behaves

like $-\sqrt{5}\varphi^k/2$, so that it is highly oscillatory. This explains intuitively the second weak convergence in (7.8).

Let us consider now $y^1 \in H^{-1}(0,1)$, $y^1(x) = \sum_{k\geq 1} \widehat{y}^{k,1}\varphi^k(x)$, with $||y^1||^2_{H^{-1}} = \sum_{k\geq 1} |\widehat{y}^{k,1}|^2/(k\pi)^2 < \infty$. Using the Riesz Representation Theorem (cf. [3], Theorem 5.5, pp. 135), there exists $\widetilde{y}^1 \in H_0^1(0,1)$ such that $\langle y^1, \phi\rangle_{H^{-1},H_0^1} = (\widetilde{y}^1, \phi)_{H_0^1}$ and $||y^1||_{H^{-1}} = ||\widetilde{y}^1||_{H_0^1}$, with $\widetilde{y}^1(x) = \sum_{k\geq 1} \widehat{y}^{k,1}\varphi^k(x)/(k\pi)^2$. We construct firstly the projection of $\widetilde{y}^1 \in H_0^1(0,1)$ on $\mathcal{U}_h$ given by

$$\widetilde{y}_h^1(x) := \sum_{k=1}^{N} \left( \frac{(\widetilde{y}^1, \varphi_h^{a,k})_{H_0^1}}{\Lambda_h^{a,k}} \varphi_h^{a,k}(x) + \frac{(\widetilde{y}^1, \varphi_h^{o,k})_{H_0^1}}{\Lambda_h^{o,k}} \varphi_h^{o,k}(x) \right) + \frac{(\widetilde{y}^1, \varphi_h^{r})_{H_0^1}}{\Lambda_h^{r}} \varphi_h^{r}(x).$$

Then, in order to find the approximation $y_h^1 \in \mathcal{U}_h$ of $y^1$, we solve $\langle y_h^1, \phi_h\rangle_{H^{-1},H_0^1} = (\widetilde{y}_h^1, \phi_h)_{H_0^1}$ for all $\phi_h \in \mathcal{U}_h$. But, since $y_h^1 \in \mathcal{U}_h \subset L^2(0,1)$, $\langle y_h^1, \phi_h\rangle_{H^{-1},H_0^1} = (y_h^1, \phi_h)_{L^2}$, so that $y_h^1$ has the representation (7.10), with $\widehat{y}_h^{\alpha,k,1} = (\widetilde{y}^1, \varphi_h^{\alpha,k})_{H_0^1} = \langle y^1, \varphi_h^{\alpha,k}\rangle_{H^{-1},H_0^1}$ and $\widehat{y}_h^{r,1} = (\widetilde{y}^1, \varphi_h^{r})_{H_0^1} = \langle y^1, \varphi_h^{r}\rangle_{H^{-1},H_0^1}$, i.e. (7.11). In fact, the coefficients $\mathbf{Y}_h^1$ and $\widetilde{\mathbf{Y}}_h^1$ of $y_h^1$ and $\widetilde{y}_h^1$ with respect to the basis $(\phi_{j/2})_{1\leq j\leq 2N+1}$ in Fig. 2.1 satisfy the identity $\mathbf{Y}_h^1 = M_h^{-1} S_h \widetilde{\mathbf{Y}}_h^1$. Since $\widetilde{y}_h^1$ is the projection of $\widetilde{y}^1 \in H_0^1(0,1)$ on $\mathcal{U}_h$, we get

$$||\mathbf{Y}_h^1||_{\mathcal{H}_h^{-1}} = ||\widetilde{\mathbf{Y}}_h^1||_{\mathcal{H}_h^1} = ||\widetilde{y}_h^1||_{H_0^1} \leq ||\widetilde{y}^1||_{H_0^1} = ||y^1||_{H^{-1}}. \tag{7.30}$$

The expression of $\widehat{y}_h^{\alpha,k,1}$ is similar to the one of $\widehat{y}_h^{\alpha,k,0}$ in (7.28), so that, since $\lambda_h^{a,k} \to k\pi$, we get $\widehat{y}^{a,k,1}/\lambda_h^{a,k} \to \widehat{y}^{k,1}/(k\pi)$. Also $1/\lambda_h^{o,k} \to 0$ and therefore $\widehat{y}^{o,k,1}/\lambda_h^{o,k} \to 0$ as $h \to 0$ for fixed $k \in \mathbb{N}$. These remarks combined with the bound in (7.30) conclude the first convergence in (7.7) and (7.8).

In order to obtain strong convergence in (7.7) and (7.8), we prove in a similar way that, for $y_h^0$ and $y_h^1$ of Fourier coefficients given by (7.12), the weak convergence in (7.7) and (7.8) holds in $\hbar^1 := \{(f_j)_{j\geq 1} \in \ell^2, \sum_{j\geq 1} j^2|f_j|^2 < \infty\}$. The strong convergence in $\ell^2$ holds since $\hbar^1$ is compactly embedded in $\ell^2$. □

**8. Final comments and open problems.** In this paper, we do a careful analysis of the numerical pathologies that might occur when approximate the 1-d controlled wave equation and its adjoint system by $P_2$-finite elements. We design several filtering mechanisms for the initial data in the discrete adjoint problem based on the Fourier truncation method and on the bi-grid algorithm and prove their efficiency. In the last part of this article, we prove the convergence to the continuous HUM control of the discrete controls obtained by minimizing the functional $\mathcal{J}_h$ in (2.12) over the restricted space of Fourier truncated or of bi-grid data.

The main difficulty to study the $P_2$-finite element approximation of the control problem with respect to previous analyzed methods (finite differences or $P_1$-finite elements, see [9] or [26]) is generated by the presence of the added optic branch of the spectrum. This spurious mode is not an inconvenient for the convergence of the method in the classical sense of numerical analysis, but it adds two new points of vanishing spectral gap as $h \to 0$ to the one on the acoustic diagram. This is an added drawback for the uniform observability to hold. The Fourier truncation method, whose efficiency is justified by a classical result of Ingham (cf. [19]), is computationally expensive in practice. Its use can be avoided by implementing R. Glowinski's bi-grid method introduced in [10]. The main contribution of this paper is to present an adaption of this two-grid strategy to the the $P_2$-approximation under

consideration, in which the spectrum is more complex and has several wave numbers of vanishing group velocity. The optic mode of the spectrum is generated by the dynamics of the values of the numerical solution at the midpoints of the grid. Thus, the most natural strategy to attenuate the pathologies generated by the optic mode is to restrict the class of initial data to linear ones in each computational cell. The proof of the convergence of this remedy follows the methodology in [16].

In [9], it was proved that, for initial data $(y^0, y^1) \in H_0^1 \times L^2(0,1)$ in the continuous control problem (1.1), the numerical controls obtained for the finite difference or the linear finite element semi-discretization of the wave equation (1.1) by minimizing the discrete quadratic functional over a filtered space converge to the continuous HUM controls with an error order $h^{2/3}$. This is due to the fact that $|\lambda_h(\xi) - \xi| \sim h^2\xi^3$, where $\lambda_h(\xi)$ can be each one of the dispersion relations for the finite difference or finite element approximation of the wave equation. It is well-known (cf. [2]) that the accuracy of the finite element method increases with the order of the polynomial in the approximation. Indeed, one can easily check that the acoustic dispersion relation $\lambda_h^a(\xi)$ of the $P_2$ - finite element method approximates the continuous one $\xi$ with an error of order $h^4\xi^5$ for all $\xi \in [0, \pi/h]$, so that the convergence error for the numerical controls obtained by the bi-grid algorithm in the quadratic approximation of the wave equation increases to $h^{4/5}$ under the regularity assumption $(y^0, y^1) \in H_0^1 \times L^2(0,1)$ on the continuous initial data to be controlled. In fact, in [22] we observed numerically this improvement in the convergence rate for the numerical controls when passing from piecewise linear to quadratic finite element approximations.

All the results in this paper can be extended to finite element methods of arbitrary order $k$, with the additional difficulty that when computing the eigenvalues, the quadratic equation (3.8) has to be replaced by a $k$-th order algebraic equation in $\Lambda$ which is technically complicated to be solved explicitly. The same difficulty arises when passing to several space dimensions on triangular uniform meshes. As we saw in Section 3, one can do an explicit Fourier analysis for the biquadratic finite element approximation of the 2-d wave equation on quadrilateral uniform meshes in each direction. In that case, it is expected that, by minimizing the corresponding discrete quadratic functional over an appropriate filtered subspace (obtained for example by applying a bi-grid technique as in [16] to linear data), the convergence of the optimal controls in the biquadratic finite element approximations of the 2-d controlled wave equation to the continuous HUM controls can be achieved.

The results in [8] providing a general method to obtain uniform observability results for time discretizations of conservative system lead to the extension of our observability results for the $P_2$ - space semi-discretization to fully discrete $P_2$ conservative approximations of the wave equation.

The extension of the results in this paper to non-uniform meshes is a completely open problem.

The last open problem we propose is to design appropriate bi-grid algorithms taking care of all the singularities of both group velocity and acceleration simultaneously and ensuring the dispersive properties of the Schrödinger equation approximated in space using the $P_2$ - finite element method to hold uniformly as $h \to 0$ (see [15] for the case when the Schrödinger equation is approximated by finite differences).

**Acknowledgements.** Both authors wish to thank S. Micu (University of Craiova) and S. Ervedoza (Institut de Mathématiques de Toulouse) for fruitful discussions.

REFERENCES

[1] Ainsworth M., *Discrete dispersion relation for hp-version finite element approximation at high wave number*, SIAM J. Numer. Anal., 42(2004), 553–575.
[2] Bowles J. B., Vichnevetsky R., *Fourier analysis of numerical approximations of hyperbolic equations*, SIAM Atudies in Applied Mathematics, 1982.
[3] Brezis H., *Functional analysis, Sobolev spaces and partial differential equations*, Springer, 2010.
[4] Castro C., Micu S., *Boundary controllability of a linear semi-discrete 1-d wave equation derived from a mixed finite element method*, Numer. Math., 102(3)(2006), 413–462.
[5] Dacorogna B., *Direct methods in the calculus of variations*, Springer-Verlag, 1989.
[6] Ervedoza S., *Spectral conditions for admissibility and observability of wave systems*, Numer. Math., 113(3)(2009), 377–415.
[7] Ervedoza S., *Admissibility and observability for Schrödinger systems: Applications to finite element approximation schemes*, Asymptot. Anal., 71(1)(2011), 1–32.
[8] Ervedoza S., Zheng C., Zuazua E., *On the observability of time-discrete conservative linear systems*, J. Functional Analysis, 254(12)(2008), 3037–3078.
[9] Ervedoza S., Zuazua E., *The wave equation: control and numerics*, in Control and stabilization of PDEs, P. M. Cannarsa and J. M. Coron eds., Lecture Notes in Mathematics, CIME Subseries, Springer Verlag, Vol. 2048, 2012, 245–339.
[10] Glowinski R., *Ensuring well posedness by analogy: Stokes problem and boundary control for the wave equation*, J. Comput. Physics, 103(2)(1992), 189–221.
[11] Glowinski R., Li C. H., Lions J. L., *A numerical approach to the exact boundary controllability of the wave equation. I. Dirichlet controls: description of the numerical methods*, Japan J. Appl. Math., 7(1)(1990), 1–76.
[12] Graham A., *Kronecker products and matrix calculus with applications*, Ellis Horwood, 1981.
[13] Gugat M., *Penalty techniques for state constrained optimal control problems with the wave equation*, SIAM J. Control Optim., 48(5)(2009), 3026–3051.
[14] Hughes T. R. J., Reali A., Sangalli G., *Duality and unified analysis of discrete approximations in structural dynamics and wave propagation: Comparison of p-method finite elements with k-method NURBS*, Comput. Meth. Appl. Mech. Eng., 197(49- 50)(2008), 4104–4124.
[15] Ignat L., Zuazua E., *Numerical dispersive schemes for the nonlinear Schrödinger equation*, SIAM J. Numer. Anal., 47(2)(2009), 1366–1390.
[16] Ignat L., Zuazua E., *Convergence of a two-grid algorithm for the control of the wave equation*, J. Eur. Math. Soc., 11(2)(2009), 351–391.
[17] Infante J.-A., Zuazua E., *Boundary observability for the space semidiscretization of the 1-d wave equation*, M2AN, 33(1999), 407–438.
[18] Lions J. L., *Contrôlabilité exacte, perturbations et stabilisation des systèmes distribués*, vol. 1, Masson, Paris, 1988.
[19] Loretti P., Komornik V., *Fourier series in control theory*, Springer, 2004.
[20] Loreti P., Mehrenberger M., *An Ingham type proof for a two-grid observability theorem*, ESAIM: COCV, 14(3)(2008), 604–631.
[21] Marica A., Zuazua E., *Localized solutions and filtering mechanisms for the discontinuous Galerkin semi-discretizations of the 1-d wave equation*, C. R. Acad. Sci. Paris Ser. I, 348(2010), 1087–1092.
[22] Marica A., Zuazua E., *On the quadratic finite element approximation of 1-d waves: propagation, observation, control and numerical implementation*, Proceedings of "CFL-80: A Celebration of 80 Years of the Discovery of CFL Condition", C. Kubrusly and C. A. Moura, eds., Springer Proceedings in Mathematics, Springer Verlag, to appear.
[23] Micu S., *Uniform boundary controllability of a semidiscrete 1-d wave equation with vanishing viscosity*, SIAM J. Control Optim., 47(6)(2008), 2857–2885.
[24] Negreanu M., Zuazua E., *Convergence of a multigrid method for the controllability of a 1-d wave equation*, C. R. Math. Acad. Sci. Paris, 338(2004), 413–418.
[25] Tcheugoué Tébou L.R., Zuazua E., *Uniform boundary stabilization of the finite difference space discretization of the 1-d wave equation*, Advances Comput. Math., 26(2007), 337–365.
[26] Zuazua E., *Propagation, observation, control and numerical approximations of waves*, SIAM Review, 47(2)(2005), 197–243.